Reelin Controls the Directional Orientation, Apical Localization and Length of Primary Cilia in Principal Neurons in the Cerebral Cortex

Sumaya Akter[1], Soheila Mirhosseiniardakani[1], Yuto Takekoshi[3], Liyan Qiu[1], Kevin Baker[1], Kevin Jiang[1], Mark Lyon[2], Mitsuharu Hattori[3,*] and Xuanmao Chen[1,*]

[1]Department of Molecular, Cellular, and Biomedical Sciences; College of Life Sciences and Agriculture, University of New Hampshire, 46 College Road, Durham, NH 03824. [2]Department of Mathematics and Statistics, College of Engineering and Physical Sciences, University of New Hampshire, Durham, NH 03824. [3]Department of Biomedical Science, Graduate School of Pharmaceutical Sciences, Nagoya City University, Nagoya, Aichi 467-8603, Japan. *Correspondence should be addressed to Mitsuharu Hattori, email: mhattori@phar.nagoya-cu.ac.jp or Xuanmao Chen, email: Xuanmao.Chen@unh.edu

Running Title: Reelin Influences Ciliation Patterns

Key Words: Primary Cilia, Reelin, Postnatal Neuron Positioning, Cilia Orientation, Reverse Movement, Apical-Basal Neuron Polarity

The authors declare no competing financial interests

Funding and Acknowledgments: This research was supported by National Institutes of Health Grants P20GM113131-7006, R15MH126317, and R15MH125305 to X.C.; and by UNH CoRE awards, Cole Neuroscience and Behavioral Faculty Research Awards, and a COLSA Community of Teaching and Research Scholar Award (to X.C.); Grants-in-aid for Scientific Research of Japan Society for Promotion of Science JP24KJ1889 to Y.T.; Grants-in-aid for Scientific Research of Japan Society for Promotion of Science JP20H03384 and JP23K27324 (to M.H).; Grant-in-Aid for Outstanding Research Group Support Program in Nagoya City University (Grant Number 2401101). S.A. and S.M. were funded by UNH Summer TA Research Fellowships (STAF), K.B. by a McNair Scholar Award, and K.J. by an Undergraduate Research Award at UNH. We are grateful to the University Instrumentation Center at UNH for A1R HD confocal imaging service.

This manuscript contains 29 text pages, 9 Figures, 2 Supplemental Tables and 4 Supplemental Figures

Abstract

The primary cilia of pyramidal neurons in inside-out laminated regions orient predominantly toward the pia, reflecting reverse soma movement during postnatal neurodevelopment. However, the mechanisms underlying the directional cilia orientation are unknown. Here we show that the primary cilia of pyramidal neurons are localized near the base of the apical dendrites and aligned on the nuclear side opposite to the axon initial segment (AIS). However, this pattern is not observed in atypical pyramidal neurons in the deep neocortex, excitatory neurons in non-laminated regions, interneurons, or astrocytes, where cilia are irregularly positioned around the nuclei and lack preferred orientation. In Reelin-deficient mice (*reeler*), the directional orientation and apical location of cilia in late-born neocortical and CA1 neurons are disrupted. However, the initial impairments are partially corrected during postnatal development, along with a realignment of apical-basal orientation. In contrast, loss of Reelin drastically disrupts the directional orientation of cilia in early-born neocortical neurons and principal neurons in evolutionarily conserved cortical regions, which lack postnatal correction. Consistently, their cilia do not preferably localize to the apical side. Additionally, Reelin deficiency increases the cilia length of principal neurons across the cerebral cortex at a developmental stage when cilia stabilize in wild-type mice, but this effect is not observed in interneurons, astrocytes, or excitatory neurons in non-laminated regions. Together, Reelin controls the directional orientation, apical localization, and length of primary cilia in principal neurons in the cerebral cortex, underscoring the cilium as a key apical domain particularly prominent in late-born neurons.

Introduction

The extracellular matrix protein Reelin is a crucial determinator directing neuronal migration of principal neurons and lamina formation in the cerebral cortex (Alexander et al., 2023; Hattori, 2025; Jossin, 2020). Reelin exerts its effects through binding to two lipoprotein receptors, ApoER2 and VLDLR, initiating a signaling cascade involving the phosphorylation of the adaptor protein Dab1 (Frotscher et al., 2009; Trommsdorff et al., 1999). By modulating cytoskeleton dynamics, stabilizing leading process, and regulating soma translocation (Jossin, 2020), Reelin influences the establishment and maintenance of apical-basal polarity of principal neurons in the cerebral cortex (Kupferman et al., 2014; Matsuki et al., 2010). Disruption of Reelin or its essential downstream signaling proteins, as seen in Reelin null mutant *reeler* (D'Arcangelo et al., 1995), ApoER2 and VLDLR double knockouts (Frotscher et al., 2009; Trommsdorff et al., 1999), or Dab1 null mutant mice (Howell et al., 1997; Sheldon et al., 1997; Yoneshima et al., 1997), results in abnormal neuronal morphology, apical-basal misorientation, and profoundly disorganized cortical formations. These changes are associated with numerous downstream consequences, including synaptic dysfunction and severe neurological disorders such as lissencephaly, ataxia, and schizophrenia and neurodegeneration (Alexander et al., 2023; Hattori, 2025; Ishii et al., 2016; Joly-Amado et al., 2023; Jossin, 2020; Katsuyama and Hattori, 2024; Stranahan et al., 2013). While Reelin is known to guide embryonic neuronal migration and cortical formation (Alexander et al., 2023; Jossin, 2020; Katsuyama and Hattori, 2024), its roles in postnatal neuronal positioning and underlying mechanisms are not fully understood.

Primary cilia are centriole-derived organelles that are expressed in nearly all mammalian cells (Bishop et al., 2007; Sterpka and Chen, 2018; Wilsch-Bräuninger and Huttner, 2021; Yang et al., 2025). Cilia length vary greatly across brain regions, developmental stages, day and night rhythm, as well as

metabolic or disease conditions (Macarelli et al., 2023; Phua et al., 2019; Sterpka et al., 2020; Tu et al., 2023; Yang et al., 2025). Altered ciliary signaling affects neurodevelopment, leading to various ciliopathies such as cortical malformation, cognitive deficits, and behavioral abnormalities (Green and Mykytyn, 2014; Hasenpusch-Theil and Theil, 2021; Lee and Gleeson, 2011; Singla and Reiter, 2006). During embryonic neurodevelopment, primary cilia coordinate key signaling pathways such as the sonic hedgehog signaling (Bangs and Anderson, 2017; Breunig et al., 2008; Ho and Stearns, 2021) and WNT signaling (Niehrs et al., 2025; Vuong and Mlodzik, 2023), and regulate multiple developmental processes (Valente et al., 2014), including cell fate determination (Jang et al., 2016; Yanardag and Pugacheva, 2021) and dorsal-ventral patterning of the neural tube (Pal and Mukhopadhyay, 2015; Sasai and Briscoe, 2012). However, specifically the primary cilia of principal neurons in the cerebral cortex do not arise during the embryonic stage (Yang et al., 2025). The full emanation of primary cilia out of the centrioles that occurs postnatally, varying from P3 to P14 and depending on animal strains and brain regions, may reflect the dynamic process of postnatal neuron positioning. We have previously analyzed cilia morphology and directionality in the postnatal mouse brain and found after postnatal day 14 (P14), the primary cilia of principal neurons in inside-out laminated brain regions spanning from the hippocampal CA1 region to neocortex are predominantly oriented toward the pial surface (Yang et al., 2025). Along with other converging evidence, the directional orientation of cilia reflects a slow “reverse movement” of late-born pyramidal neurons during postnatal positioning (Yang et al., 2025).

In this study, we initially found that the cilia bases (or centrioles) of principal neurons, particularly late-born pyramidal neurons, in the cerebral cortex are localized near the base of the apical dendrites, aligning opposite to AIS in reference to the nucleus. However, this phenomenon is not observed in atypical pyramidal neurons in the deep neocortex, excitatory neurons in the amygdala and other nucleated brain regions or interneurons. Yet, it is unknown which factor controls cilia

directionality and apical localization in principal neurons in the cerebral cortex. Given Reelin guides neuronal migration and strongly influences the neuronal polarity of pyramidal neurons (D'Arcangelo et al., 1995; Kupferman et al., 2014; Matsuki et al., 2010), we tested the hypothesis that Reelin dictates cilia directionality and cilia apical localization in principal neurons. Using Reelin null mutant mice (*reeler*) (Curran et al., 1995; D'Arcangelo et al., 1995; Falconer, 1951; Ogawa et al., 1995), we discovered that Reelin indeed influences cilia directional orientation and cilia localization to the base of apical dendrites of pyramidal neurons in the cerebral cortex. Surprisingly, Reelin deficiency affects early-born neurons and principal neurons in the piriform cortex, CA3 and DG more severely than late-born principal neurons with respect to cilia orientation, cilia apical localization or apical-basal neuronal orientation. In addition, Reelin deficiency also promotes cilia elongation in principal neurons throughout the cerebral cortex after P14, a developmental stage when primary cilia stabilize in WT mice (Yang et al., 2025). However, Reelin does not affect cilia length in interneurons, astrocytes, or excitatory neurons in nucleated brain regions. In conclusion, Reelin controls the directional orientation, intracellular localization, and length of primary cilia in principal neurons in the cerebral cortex. These data also demonstrate that primary cilia represent a key apical signaling domain in pyramidal neurons.

Methods and Materials

Animals

Mice were housed under a 12-hour light/dark cycle (lights on from 6:00 A.M. to 6:00 P.M.) and provided with standard chow and water ad libitum. Crl:CD-1 mice (RRID: MGI:5652673) were obtained from Japan SLC. *Reeler* mice (B6C3Fe a/a-Reln^{rl} /J, RRID: IMSR_JAX:000235) were obtained from the Jackson Laboratory and backcrossed to the Crl:CD-1 strain. Both male and female

mice were used in all experiments. Mice were fixed with 4% paraformaldehyde (PFA) in phosphate-buffered saline (PBS) by intracardiac perfusion. The brains were post-fixed with 4% PFA in PBS overnight before dehydration using 30% sucrose. If not otherwise indicated, experiments were performed using wild-type mice with C57BL/6j genetic background. All animal procedures were approved by the Institutional Animal Care and Use Committee of the University of New Hampshire (Approved Numbers: 191102 and 221202) or by the Animal Care and Use Committee of the Nagoya City University and conducted in accordance with the Institutional Guidelines for Animal Experimentation (Approval Number: 23-001H05).

Immunofluorescence Staining

Mouse brains were sliced and mounted on gelatin-coated slices for doing immunostaining method. They were washed three times with 0.1 M PBS. Then they were washed in 0.2% Triton X-100 (vol/vol) in 0.1 M PBS three times for 10 minutes at room temperature. Then they were blocked in blocking buffer (0.1M PBS containing 10% normal donkey serum (vol/vol), 2% bovine serum albumin (weight/vol), 0.2% Triton X-100 (vol/vol)) for 1-2 h at room temperature. After that, slices were incubated with primary antibodies overnight at 4 °C in blocking buffer. After washing in 0.1 M PBS three times for 10 minutes, slices were incubated with secondary antibodies for 2 hours at room temperature. Primary antibodies were rabbit anti-AC3 (1:10000 dilution, EnCor Biotechnology Inc., #RPCA AC3) or chicken anti-AC3 (1:1000 EnCor Biotechnology Inc., Cat# CPCA-ACIII), Rabbit anti-Glutaminase I (1:500, Synaptic Systems #456003), rat anti-Ctip2 (1:500, Millipore-Sigma, MABE1045), rabbit anti-Satb2 (1:500, Abcam, ab92446), mouse anti-Ankyrin G (1:500, Synaptic System, #181011), and mouse anti-NeuN (1:500, Millipore-Sigma, MAB377, clone A60). Secondary antibodies were mostly from Donkey conjugated with Alexa Fluor 488, 546, or 647 (Invitrogen, La Jolla, CA). Finally, sections were counter-

stained with DAPI (Southern Biotech, #OB010020) and images were acquired with confocal microscope (Nikon, A1R-HD), installed in the University Instrument Center.

Cilia Orientation Measurement

Cilia orientation of early-born neurons was measured based on immunostaining of CTIP2 and AC3 antibodies. Cilia orientation of late-born neurons was measured based on immunostaining of Satb2 and AC3 antibodies. Cilia orientation of excitatory neurons was measured based on immunostaining of Glutaminase I and AC3 antibodies. GFAP and GAD65 antibodies were employed in immunostaining to differentiate astrocyte and interneurons. We used custom-made MATLAB Apps, named Cilia Locator and Cilia Analysis, to identify cilia in confocal images and determine cilia directionality (Yang et al., 2025) and (Mirhosseiniardakani et al., 2025). Collected data were exported into Excel file and then to a MATLAB program, which was used to generate polar plots, histogram and fit histogram.

Primary Cilia Length Measurement

We assessed the primary cilia length following published methods (Sipos et al., 2018), with modifications. Cilia length was measured using the freehand line tool within Fiji (ImageJ) from the base of axoneme to the distal tip.

Cilia and Axon Quadrant Analysis

NeuN and Glutaminase I immunostaining revealed the shapes of apical dendrites of principal neurons, which allowed cilia location identification. To evaluate the spatial distribution of primary cilia and axons in various cell types and different brain regions, high-resolution confocal images were acquired using a 40X oil-immersion objective in Nikon’s Confocal microscope. Each soma/cell body was subdivided into four quadrants like apical, basal, left lateral, and right lateral by drawing perpendicular lines in Fiji (ImageJ) intersecting at the center of nuclear centriole, aligned with the apical–basal axis of the neuron.

For interneurons and astrocytes which may not aways have a primary dendrite, we separate each cell body into four quadrants (top, bottom, left lateral, and right lateral). Each cilium base or axons position was determined based on the quadrant in which the majority of the ciliary axoneme was localized. For each location, a minimum of 100 cells per condition were analyzed across multiple sections and animals. The percentage of cilia/axon in each quadrant was calculated and compared to determine whether they were equally distributed among the four orientations.

Cilia Orientation Analysis Software and General Statistics

Data analysis was conducted using Fiji, GraphPad Prism and presented using CorelDRAW. A custom-made MATLAB App was developed to analyze cilia orientation. The software utilized MATLAB's custom distribution fitting algorithms to facilitate the fitting of the orientation data to several different distribution models (uniform distribution - irregular cilia orientation; mono periodic normal distribution - one major cilia orientation; and double periodic normal distribution - two cilia orientations). The Kolmogorov - Smirnov tests were applied to test the hypothesis that sampled orientation distribution could have been drawn from the fit probability distribution and facilitated the plotting of both the sampled orientation distribution and fit probability distribution. General statistical analyses were performed using independent two-sample Student's t-tests to evaluate statistical significance between the WT and *reeler* groups, with a significance threshold of $p < 0.05$. Unless otherwise specified in the text or figure legends, significance levels are indicated as follows: ns (not significant); * $p < 0.05$; ** $p < 0.01$; *** $p < 0.001$. Statistical significance was determined in the graph at $p < 0.05$, with values presented as mean ± standard error of the mean (SEM). Data were collected from multiple sections from three or more mice (mixed sex) for each group, if not otherwise indicated.

Results

Primary Cilia of Pyramidal Neurons in Inside-out Laminated Regions are Localized near the Base of the Apical Dendrites.

To examine the spatial relationship between cilia base (or centriole) location, cilia orientation, and the apical dendrites in the WT neocortex, we performed immunofluorescence staining on fixed WT brain sections using AC3 antibodies, an established cilia marker (Bishop et al., 2007; Chen et al., 2016; Zhou et al., 2019), along with cell type-specific markers. We systematically assessed the orientation and intracellular location of primary cilia in various cell types and brain regions of mice.

Firstly, we found that cilia were consistently localized near the base of the apical dendrites of pyramidal neurons in all inside-out laminated brain regions, which include the neocortex (except for atypical pyramidal neurons), entorhinal cortex, cingulate cortex, hippocampal CA1, and piriform cortex (Fig. 1A-B, Table S1). Intriguingly, the cilia intracellular location is consistent with their cilia orientation predominantly toward the pial surface, align opposite to AIS relative to the nuclei (Fig. 1C-D). We also compared principal neurons in superficial and deep cortical layers at P30. In both layers, the bases of cilia were mostly positioned near the base of the apical dendrites, with primary cilia directing in the same pia direction. Notably, the pattern of cilia-at-apical while axon-at-basal is most striking among late-born pyramidal neurons in the neocortex and CA1, compared to early-born neocortical neurons and other cell types. This is in line with stronger cilia orientation toward the pial surface in late-born neurons (Figure 1C-D).

Secondly, atypical pyramidal neurons in the deep neocortex, which deviate from the classical morphological and electrophysiological features of pyramidal neurons (Landrieu and Goffinet, 1981), and some have inverted, while others have oblique apical dendrites (Steger et al., 2018; Steger et al.,

2013). Immunostaining for AC3, Glutaminase I (or NeuN) and DAPI revealed abundant cilia in these cells (Fig. S1). However, cilia orientation exhibits an irregular pattern. The histogram of angular frequency demonstrated a broad, evenly dispersed distribution without dominant peak (Fig. S1C), indicating a lack of preferred orientation. This was further confirmed by the color-coded spatial maps of cilia orientation (Fig. S1D), which showed diverse angular values. The analysis of cilia subcellular location (Fig. S1E) also revealed even distribution of cilia among four quadrants, supporting the absence of location bias. Hence, unlike pyramidal neurons in laminated regions, atypical pyramidal neurons in the WT deep neocortical layer do not display directional cilia orientation or preferred apical localization.

Thirdly, pyramidal or excitatory neurons in the amygdala are non-laminated but organized into distinct nuclei (LeDoux, 2007). Their cilia distribution pattern somewhat resembled that of atypical pyramidal neurons in the deep neocortex: primary cilia do not preferably localize to the base of the apical dendrites (the apical quadrant) and cilia lack specific orientation (Fig. S2). Consistently, in other non-laminated brain regions examined, such as the hypothalamus, striatum, and thalamus, the cilia of excitatory neurons were randomly positioned around the soma near the nucleus, showing no consistent directional orientation (Table S1).

Fourthly, primary cilia of interneurons and astrocytes throughout the brain were irregularly distributed around the nucleus (Table S1) (Fig. S2F-G) and their cilia did not exhibit a directional orientation (Yang et al., 2025). Together, the primary cilia of pyramidal neurons in inside-out laminated brain regions generally localize near the base of apical dendrites (the apical quadrant) and predominantly orient toward the pial surface, while interneurons and astrocytes, atypical pyramidal neurons, and excitatory neuron in non-laminated regions do not manifest such a pattern.

Late-born, but Not Early-born Neocortical Neurons, Exhibit Postnatal Corrections in Cilia Orientation and Apical Localization, Following Disruptions Caused by Reelin Deficiency.

Reelin is a key extracellular cue that influences neuronal placement, apical-basal neuronal polarity, and layering in the cerebral cortex (Jossin, 2020; Rice and Curran, 2001). To assess whether Reelin influences the cilia orientation of primary cilia of cortical pyramidal neurons, we examined cilia directionality in the outer layer of the neocortex in WT and *reeler* mice at P30. *Reeler* carries a mutation in the Reelin gene (*Reln*) and is an extensively characterized null model (D'Arcangelo et al., 1995). We found that primary cilia in WT mice exhibited a predominant orientation toward the pial surface (Fig. 2A). Quantitative analysis of cilia orientation (Fig. 2A-C left) showed a strong peak around 90°, with most WT cilia aligned toward the pia. In contrast, *reeler* outer layer neurons showed disrupted cilia orientation, with no predominant alignment toward the pial surface (Fig. 2A-B right). The corresponding histogram of cilia orientation (Fig. 2C right) revealed a more dispersed distribution of cilia angles, lacking the distinct peak. Fitting the data with periodic normal distribution functions indicated that while WT cilia orientation followed a single periodic normal distribution centered around 90°, while the *reeler* data better fit a uniform distribution, indicative of randomized cilia orientation. Color-coded spatial maps (Fig. 2D) further supported this observation: WT samples showed a pattern with similar cilia orientation (mostly red or 90 degree), while *reeler* samples exhibited a more heterogeneous and disorganized orientation pattern throughout the outer layer.

Nevertheless, *Reeler* is known to exhibit “outside-in” or “inverted” cortical lamination and the outer layer of *reeler* mostly contains early-born neurons, while its inner layer has late-born neurons (D'Arcangelo et al., 1995; Ogawa et al., 1995), although the layer-specific boundary of *reeler* is not as sharp as WT (Hoffarth et al., 1995). To clearly distinguish early-born from late-born neurons, we used a

Ctip2 antibody and a Satb2 antibody to label early- and late-born neurons, respectively. We also analyzed the apical-basal orientation of *reeler* neocortical neurons by examining cilia's apical location and axon's basal location of P10 and P30. An ankyrin G antibody was used to label the AIS. At P10, both *reeler* early- and late-born neurons displayed random cilia orientation, irregular apical location, and disorganized axon initial segments (Fig. 3A-B). Cilia and AIS did not align opposite to each other relative to nuclei (Fig 3A-B). However, at P30, late-born *reeler* neurons manifested a remarkable improvement in cilia apical localization, orientation preference as well as relative separation between cilia and axon (Fig. 3D). In contrast, the change in early-born *reeler* neurons was much weaker: their cilia still lack a major orientation or preference in intracellular location, and the relative position from cilia to axon remains irregular (Fig. 3C). Statistical analysis of cilia location and AIS location confirmed the observations (Fig. 3E-G). This suggests that early- and late-born neurons respond differentially to Reelin deficiency. Late-born neurons are more resistant to the impairments, as they show strong postnatal corrections in apical-basal neuronal orientation.

To validate progressive corrections in neuronal orientation in *reeler* late-born neurons, we measured cilia orientation of late-born neurons (marked by Satb2) in the *reeler* neocortex at P5, P10, P14, and P30 and analyzed cilia directionality and cilia location (Fig. 4). At P5, cilia orientation was broadly distributed, with no dominant directional preference, suggesting early postnatal disorganization (Fig. 4Ai-iii). The histogram showed a minor peak oriented toward to the ventricular zone, and a flat distribution, indicating randomized cilia orientation (Fig. 4A-iv). At the same time, cilia were evenly distributed to 4 quadrants (Fig 4A-v). From P10 to P14, the angular distribution began to shift, with more cilia aligning between 70° and 110°, corresponding to orientation generally toward the pial surface. However, substantial variability remained, and the distribution lacked the sharp unimodal peak typically observed in WT mice. By P30, cilia orientation became more focused, with a clearer peak near

90°, suggesting preferred alignment toward the pia, though some cilia still deviated from this axis. Simultaneously, cilia became increasingly localized to the apical quadrant (Fig. 4B-D). These findings suggest that while cilia orientation remains imperfectly aligned, directional organization of primary cilia of *reeler* late-born neurons emerges over time due to postnatal corrections.

In contrast, primary cilia of reeler early-born neocortical neurons, marked by CTIP2 (Fig. 5C&F), maintain irregular orientation and random apical location at both P5 and P30, indicating that *reeler* early-born neurons do not undergo postnatal corrections in cilia orientation and apical-basal orientation from P5 to P30 (Fig. 5A-H). A diagram in Fig. 5I summarizes observed differences in WT and *reeler* of P30.

Reelin Deficiency Partially Affects the Apical Localization and Directional Orientation of Primary Cilia in CA1 Principal Neurons.

To examine how Reelin impacts ciliation pattern in the hippocampal CA1 region during postnatal development, we analyzed cilia orientation in WT and *reeler* CA1 region at P10, P14, and P30. In the CA1 stratum pyramidale (SP) of WTs, primary cilia exhibit one major orientation toward the pia and one weak orientation toward the opposite direction (Fig. 6A, C and E), in line with our previous report (Yang et al., 2025). In contrast, *Reeler* CA1 neurons were split to “top” and “bottom” sublayers (B and D). In the top layer, cilia consistently exhibited a strong directional bias across ages from P10 - P30, with a predominant orientation centered around 270°, indicating a preferred orientation toward pia (Fig. 6F-H, left panels). In the bottom layer, cilia displayed a bimodal orientation pattern and subject to changes with age. At P10, the distribution was more diffuse, with lower and broader peaks at 98° and 274° (Fig. 6F, right panel). At P14, the peaks were present but broader, occurring at 97° and 275° (Fig.

6G, right panel). At P30, two sharp and opposing peaks were observed at approximately 95° and 273°, with nearly equal proportions of cilia oriented in each direction (Fig. 6H, right panel).

Regarding cilia location in neurons, cilia of WT CA1 principal neurons were predominantly localized to the apical dendrites (Table S1) (Fig. 6I). Nevertheless, *reeler* cilia in the CA1 initially were not preferably localized to the apical quadrant at P10, and a large portion of cilia were distributed to other quadrants (Fig. 6J). However, cilia location underwent a postnatal re-alignment in the absence of Reelin, and cilia partially restored a major distribution to the apical quadrant at P30 (Fig. 6K). WT CA1 neurons exhibit a clear cilia-at-apical and axon-at-base orientation at both P10 and P30 (Fig. 6L). Loss of Reelin altered this pattern at P10, but the apical-basal orientation was partially reinstated at P30, although the SP was still split (Fig. 6L). Together, because of corrections, Reelin deficiency partially affects cilia directional orientation and apical location in CA1 neurons.

Loss of Reelin Disrupts the Orientation and Apical Location of Cilia in Evolutionarily Conserved Cortical Regions

The piriform cortex, a major part of the olfactory cortex, is 3-layered paleocortex. The piriform cortex is formed by an inside-out manner (Martin-Lopez et al., 2019), but a more conserved cortical structure than the hippocampal CA1 and neocortex (Klingler, 2017). We examined cilia orientation and subcellular location in Layer II and III of the WT piriform cortex at P30 (Fig. 7). In Layer II, which is a compact lamina, neuronal primary cilia exhibited two major opposite directions (Fig. 7A&C), while in Layer III, which is sparsely layered, cilia had one major direction, predominately oriented toward the pial surface (Fig. 7D). Consistently, most of cilia base were localized near the base of apical dendrite (the apical quadrant) (Fig 7G). Reelin deficiency disrupted proper neuronal placement, laminated

structures, and apical-basal neuron orientation in the piriform cortex (Fig. 7B). We further found that primary cilia in the *reeler* piriform cortex no longer exhibited preferred orientation toward the pia but manifested irregular orientation (Figure 7E-F). Consistently, cilia were no longer confined to the base of the apical dendrite but became randomly distributed across the soma (Figure 7B and 7G). These data demonstrate that Reelin deficiency disrupts the directional orientation and subcellular location of neuronal primary cilia in the piriform cortex. The phenotypes of impairment were maintained at P30, suggesting no postnatal correction occurs.

We also examined ciliation pattern in DG and CA3, which are considered conserved cortical structures (Blackstad et al., 2022; Krubitzer and Seelke, 2012), relative to the CA1 and neocortex. Similarly, Reelin deficiency disrupted the lamination of principal neurons and strongly perturbed the cilia orientation and their apical location in the DG and CA3 region of P30 (Fig. 8). Together, Reelin deficiency strongly impairs the cilia orientation and cilia apical localization in principal neurons in evolutionary conserved laminated regions, including piriform cortex, DG and CA3. These cortical regions do not manifest strong postnatal corrections in apical-basal orientation in the absence of Reelin.

Primary Cilia of Excitatory Neurons in the Amygdala Exhibit Irregular Orientation and Subcellular Location, Independent of Reelin.

To investigate whether Reelin influences cilia orientation in the amygdala, a non-laminated brain region (LeDoux, 2007), we analyzed the angular distribution of primary cilia in WT and *reeler* mice at P30 (Fig. S2). Cilia orientation histograms and frequency distributions revealed that cilia in both groups exhibited broadly dispersed orientations across the full 360° range. No preferential alignment was observed in either genotype (Fig. S2). The degree of variability appeared similar in both WT and *reeler,*

suggesting random orientation of primary cilia. Consistently, their cilia were roughly equally distributed to 4 quadrants of the soma, without a preference to the apical side (Fig. S2). These findings indicate that, unlike in laminated cortical regions, the amygdala displays irregular cilia orientation. Thus, Reelin does not appear to regulate cilia orientation and subcellular location in the amygdala and other non-laminated regions analyzed (Table S1).

Primary Cilia of Principal Neurons in the *Reeler* Cerebral Cortex Continue to Elongate at a Developmental Stage when WT Cilia Stabilize.

Next, to examine if Reelin influences cilia morphology, we measured cilia length across different regions in WT and *reeler* mice. We performed staining using an AC3 antibody to specifically mark neuronal primary cilia (Bishop et al., 2007; Chen et al., 2016; Zhou et al., 2019) and Arl13b antibody to label astrocytic primary cilia (Sterpka and Chen, 2018; Sterpka et al., 2020). We analyzed cilia in WT and *reeler* mice at P14 and P30, first focusing on laminated brain structures including the hippocampal CA1, CA3, DG, superficial and deep layers of the neocortex, piriform cortex, and entorhinal cortex.

In the CA1 region, neuronal primary cilia were longer in *reeler* than in WT of P30 (Fig. 9A, left). Quantitative analysis of cilia length, as shown in the bar graph (Fig. 9A, right), confirmed a significant increase in cilia length in *reeler* mice. This trend of elongated cilia was consistently observed in all other laminated regions analyzed, including CA3, DG, superficial neocortex, deep neocortex, and piriform cortex (Fig. 9B-E, Table S2). At P14, cilia lengths in *reeler* mice were comparable to WT controls across all regions, with minor differences detected (Fig. 9B-E, P14 groups). Additionally, WT mice exhibited comparable cilia lengths between P14 and P30, consistent with previous report (Yang et al., 2025). In contrast, *reeler* mice showed a pronounced elongation of primary cilia from P14 to P30 in

all laminated brain regions examined. This age-dependent divergence suggests that Reelin or proper layering is essential for constraining cilia growth during postnatal cortical development.

Loss of Reelin does not Affect the Cilia Length of Excitatory Neurons in Non-Laminated brain Regions, Interneurons or Astrocytes.

To determine whether Reelin influences cilia morphology in non-laminated brain regions, we measured cilia length in several areas in WT and *reeler* mice of P30. These regions included the thalamus, striatum, hypothalamus, and amygdala. In the thalamus (Fig. S3A), immunofluorescence images (right panels) show similar cilia length between WT and *reeler* mice, and the corresponding bar graph (left panel) confirms no significant difference in cilia length. Likewise, in the striatum (Fig. S3B), hypothalamus (Fig. S3C), and amygdala (Fig. S3D), there are no differences in cilia length between genotypes. These findings indicate that Reelin does not affect cilia length in non-laminated regions of the brain.

To determine whether Reelin affects cilia morphology in interneurons, we measured cilia length in WT and *reeler* mice at P30 using AC3 immunostaining in combination with interneuron-specific markers GAD65 (Kajita and Mushiake, 2021). In the CA1 region of the hippocampus, there was no significant difference in interneuron cilia length between genotypes (Figure S4A). Similarly, in both the deep and superficial layers of the neocortex, cilia length in interneurons did not differ between WT and *reeler* mice (Figure S4B-C). These findings demonstrate that Reelin does not influence primary cilia morphology in interneurons.

To determine whether Reelin affects cilia length in astrocytes, we measured cilia length in WT and *reeler* mice at P30 using an Arl13b antibody co-immunostaining with astrocyte-specific marker

GFAP (Sterpka and Chen, 2018). In the CA1 region of the hippocampus, there was no significant difference in cilia length between genotypes (Figure S4D). Similarly, in both the deep and superficial layers of the neocortex, astrocytic cilia length did not differ between WT and *reeler* mice (Figure S4E-F). These findings indicate that Reelin does not affect primary cilia length in astrocytes.

Discussion

We have shown that the primary cilia of principal neurons in inside-out laminated regions, including the neocortex and CA1, are positioned to the base of the apical dendrite and aligned on the nuclear side opposite to AIS (Fig. 1, Table S1). In contrast, the primary cilia of interneurons, astrocytes, atypical pyramidal neurons in the deep neocortex, excitatory neurons in non-laminated brain regions are irregularly positioned in the soma or around the nuclei and cilia lack directional orientation (Fig. S1-2, Table S1). Because Reelin plays a critical role in neuronal positioning and cortical lamination in the mammalian cerebral cortex (Jossin, 2020), we utilized the *reeler* mouse model to investigate cilia orientation, intracellular localization, and morphology. *Reeler* is a well-characterized Reelin-deficient strain that exhibits “outside-in” cortical lamination, disrupted apical-basal orientation, and a range of other cellular and behavioral abnormalities (Curran et al., 1995; D'Arcangelo et al., 1995; Falconer, 1951; Ogawa et al., 1995).

We discovered that the primary cilia of *reeler* early-born neurons in the neocortex, and principal neurons in evolutionarily conserved regions (piriform cortex, DG and CA3) do not exhibit directional cilia orientation, nor do their cilia localize to the base of the apical dendrite (Table S1). In contrast, most *reeler* late-born neurons are initially misplaced in terms of apical-basal orientation and do not exhibit cilia directional orientation and apical location at early postnatal stage (before P14). However, a large fraction of neurons can gradually rectify cilia orientation and apical location, along with corrected apical-basal orientation, during late postnatal development. Moreover, the primary cilia in principal

neurons throughout the *reeler* cerebral cortex become longer than those of WT as age. The elongation of cilia in *reeler* aligns with observed alterations and corrections in their orientation and positioning, all of which occur in principal neurons of the cerebral cortex.

Primary Cilia Represent an Important Apical Signaling Domain of Pyramidal Neurons in the Cerebral Cortex.

This study highlights primary cilia as a defining apical feature of principal neurons in the cerebral cortex. Reelin signaling appears to play a key role in establishing this apical localization by regulating the subcellular positioning of the centrosome. As principal neurons complete their radial migration, Reelin, through activation of its receptors ApoER2 and VLDLR and subsequent downstream signaling, guides soma translocation and promotes the positioning of the centrosome near the base of the apical dendrite (Chai and Frotscher, 2016; Cooper, 2008; Jossin, 2020; Trommsdorff et al., 1999). This apical positioning of the centrosome is critical for the proper localization of the primary cilium, supporting its establishment as an apical domain of principal neurons. Thus, Reelin's influence on neuronal placement and centrosome positioning is essential for defining the spatial identity of primary cilia in the cerebral cortex.

It is well-recognized that primary cilia regulate embryonic neurodevelopment through mediating signaling pathways, such as Sonic hedgehog (Bangs and Anderson, 2017) and Wnt signaling (Niehrs et al., 2025; Vuong and Mlodzik, 2023), to regulate cell fate specification, dorsal-ventral neural tube patterning, and neurogenesis (Das and Storey, 2014; Jang et al., 2016; Su et al., 2012; Yanardag and Pugacheva, 2021). Nevertheless, the roles of primary cilia in the postnatal brain are not well understood. We show here that the primary cilia of principal neurons in the cerebral cortex are localized near the

base of the apical dendrite and predominantly orient toward the pial surface. This pattern is the most prominent in late-born neurons in the neocortex and hippocampal CA1 region, less pronounced in early born neocortical neurons and DG neurons, and not present in atypical pyramidal neurons in the deep neocortex, excitatory neurons in non-laminated brain regions, or interneurons (Figure 1 & S1-2, Table S1). This suggests that the pattern is stronger in principal neurons which are born in the late developmental stage or appear later during cortical evolution.

We also identified marked regional differences in the effects of *reeler* on cilia orientation and subcellular localization, reflecting the distinct impacts of Reelin across cortical regions. In the DG, CA3, and piriform cortex, loss of Reelin severely disrupts laminar organization; consequently, the primary cilia of principal neurons lose their apical dendritic localization and show no directional orientation (Fig. 7-8, Table S1). This phenomenon was similarly observed among early-born neurons in the neocortex (Fig. 5). However, late-born neurons in the neocortex (Fig. 3-4) and hippocampal CA1 regions (Fig. 6) exhibit certain postnatal corrections to Reelin deficiency. The primary cilia of late-born neurons in the CA1 and neocortex are postnatally corrected to be more localized to the apical dendrite and mainly orient toward the pia (Fig. 4&6).

What are the biological significances of cilia localization to the base of the apical dendrite of principal neurons, distant from AIS (Fig. 1, Table S1)? The relative distance and location of primary cilia, as signal-receiving units, and axon, as electrical output, are separated in pyramidal neurons in the cerebral cortex. In contrast, their relative locations are irregular in interneurons or excitatory neurons in non-laminated brain regions (Fig. S2, Table S1). Primary cilia function as signaling hubs that integrate extracellular cues into the soma (Valente et al., 2014). A variety of receptors including GPCRs and downstream signaling molecules have been identified in neuronal primary cilia (Mukhopadhyay and Rohatgi, 2014; Pal and Mukhopadhyay, 2015; Tschaikner et al., 2020; Wang and Ogden, 2025). A well-

defined cilia-at-apical and axon-at-basal configuration may support directional information flow and polarity maintenance along the apical-basal axis of pyramidal neurons. Additionally, this setting may avoid direct or too strong influence of ciliary input on AIS output. Given that the primary cilium of principal neurons is an apical structure, it is tempting to speculate that disruption of ciliary architecture or key ciliary signaling pathways may perturb apical synaptic connectivity or apical neuronal functions. Moreover, primary cilia not only act as sensory organelles but may also enhance the apical-basal polarity of principal neurons, particularly in late-born neurons of the cerebral cortex.

Reelin Deficiency Causes Cilia Elongation in Principal Neurons in the Cerebral Cortex.

We have shown that loss of Reelin in *reeler* leads to elongated primary cilia in principal neurons throughout the cerebral cortex, including DG, hippocampal CA1 and CA3, neocortex, piriform cortex, and entorhinal cortex (Fig. 9 and Table S2). We have previously reported that the primary cilia of principal neurons in the cerebral cortex of C57Bl6 WT mice emanate at P3-P14 during the postnatal stage (Yang et al., 2025). Cilia emanation in the cerebral cortex largely completes around P14 and cilia length does not change much afterwards (Yang et al., 2025) (Fig. 9 and Table S2). In this study, we found that the cilia length in the WT and *reeler* cerebral cortex is not markedly different at P14 (Fig. 9, Table S2), but the primary cilia of *reeler* principal neurons throughout the cerebral cortex continue to elongate after P14. The differences between *reeler* and WT thereby become stronger at P30 (Table S2).

Since Reelin regulates key processes associated with cortical layering, including neuronal migration, apical-basal polarity, and cytoskeletal dynamics (Frotscher et al., 2009; Jossin, 2020; Matsuki et al., 2010), its absence leads to impaired neuronal placement. As a result, lamination of neurons in the adult cortex is approximately inverted (Rugarli and Ballabio, 1995). Reelin functions as a stop signal for

neuronal migration during development (Frotscher et al., 2009). One explanation is that the absence of this stop signal disrupts normal developmental cues, promoting cilia elongation. An alternative explanation is that due to neuronal misplacement, *reeler* neurons continue to adjust positioning, while longer primary cilia may contribute to the re-positioning.

A clear distinction in cilia length due to Reelin deficiency was identified between laminated cortical structures and non-laminated regions. Laminated regions are strongly affected by Reelin for neuronal placement and apical-basal orientation, and most principal neurons there show directional cilia orientation, whereas neurons in nucleated regions do not. This phenotype supports the interpretation that the observed cilia elongation specifically in principal neurons in the cerebral cortex may be somewhat related to the disruption of laminar architecture. Concurrent with cilia prolongation after P14, cilia orientation and apical location in late-born neurons continue to rectify over the course of postnatal development (Fig. 2-6). As primary cilia are engaged in refining neuronal positioning (Yang et al., 2025), continued cilia elongation after P14 must be a compensatory growth. In line with this interpretation, no differences on cilia length were detected in interneurons and astrocytes throughout the WT and *reeler* brains. However, these possibilities are speculative, and further studies are needed to uncover the exact mechanisms of cilia length elongation in the absence of Reelin.

Distinct Cilia Phenotypes of Early- and Late-born Neurons in the Postnatal Brain in the Absence of Reelin

In the mammalian cerebral cortex, early- and late-born neurons differ markedly in their birthtime, laminar destiny, gene expression pattern, connectivity, and brain functions (Barbas, 2015; Cooper, 2008; Kohwi and Doe, 2013; Marin and Rubenstein, 2003). We previously reported that late-born neurons in the CA1 and neocortex undergo a slow yet substantial reverse soma movement, whereas early-born neurons exhibit this behavior to a much lesser degree, if at all (Yang et al., 2025). Because of

this difference, late-born neurons exhibit a clear cilia orientation toward the pial surface (Fig. 1D-F), whereas early-born neurons in the deep layers show more variation, though generally still directed toward the pia (Yang et al., 2025) (Fig. 1G-I).

Reelin is important not only for guiding neuronal placement but also for establishing the apical-basal orientation of principal neurons in the cerebral cortex (Kupferman et al., 2014; Matsuki et al., 2010). We have identified distinct phenotypes in cilia orientation and apical location among early-born and late-born *reeler* neocortical neurons. Reelin deficiency affects the cilia orientation and location of early-born neurons more severely than late-born neurons. Late-born neurons exhibit postnatal corrections in cilia orientation and localization, while early-born neurons do not (Fig. 2-5). Consistently, in the hippocampal CA1 region where late-born neurons prevail, *reeler* laminar structure is corrected to some degree postnatally, so does cilia apical localization (Fig. 6). However, principal neurons in the *reeler* piriform cortex behave more like early-born neurons than late-born neurons in the neocortex, and we did not detect postnatal corrections in cilia apical localization at P30 (Fig. 7). Likewise, the disruption in layering in the CA3 and DG, which are also conserved cortical regions, is very severe in *reeler* and lack marked postnatal corrections at P30 (Fig. 8).

We interpret these differences in the context of cortical evolution and postnatal neurodevelopment. Late-born neurons that emerge at later developmental stages of the cerebral cortex may acquire some new capacities, potentially enabling them to construct intricate neural networks and support higher-order brain functions. We postulate that the reversal movement, which occurs postnatally in inside-out laminated regions spanning from the hippocampal CA1 to neocortex (Yang et al., 2025), may be one of new features that late-born neurons have acquired. Besides fine-tune neuron positioning (Yang et al., 2025), the reverse movement may enhance the directional cilia orientation and apical-basal polarity of pyramidal neurons, facilitating late-born neurons to sort out information more efficiently. In

addition, the reverse movement process may enable late-born neurons to resist lamina disruption in the absence of Reelin and facilitate postnatal corrections of apical-basal misorientation. In contrast, early-born cortical neurons and principal neurons in the evolutionarily older cortical regions, such as the piriform cortex, DG and CA3, do not undergo substantial reverse movement (Yang et al., 2025) and therefor likely do not acquire this feature.

Irregular Orientation and Subcellular Localization of Primary Cilia in Atypical Pyramidal Neurons in the Deep Neocortex and Excitatory Neurons in Non-laminated Brain Regions.

All pyramidal neurons in the cerebral cortex, except for atypical pyramidal neurons in the deep neocortex, have their cilia located near the base of the apical dendrite (Table S1, Fig. S2). Why are atypical pyramidal neurons different? We reason that the birthtime of atypical pyramidal neurons may limit their exposure to Reelin. Cajal-Retzius cells begin secreting Reelin around embryonic day 10.5 (E10.5) (Hevner et al., 2003; Soriano and Del Rio, 2005). The levels and gradient strength continue to increase over time (Elorriaga et al., 2023). Layer VI neurons, among the earliest-born cortical neurons, migrate and settle in the cortical plate before the full establishment of Reelin gradients in the marginal zone (Causeret et al., 2021). As a result, these early-born neurons may be exposed to lower levels of Reelin. This weak exposure to Reelin during their migratory window may account for “inverted or atypical” neuronal orientation (Steger et al., 2018; Steger et al., 2013) and irregular cilia location and orientation in the deep neocortex (Table S1).

We also examined the cilia orientation and subcellular location of excitatory neurons in the amygdala, as well as other nucleated brain regions, and found cilia pattern resembles that of atypical pyramidal neurons in the deep neocortex (Fig. S2 and Table S1) (Yang et al., 2025). Excitatory neurons in non-laminated brain regions are not strongly affected by Reelin for neuronal placement; therefore, they do not show directional cilia orientation and preferred apical location. Furthermore, interneurons

and astrocytes also exhibit irregular cilia orientation and location (Table S1). These cell types are not laminarly structured or critically affected by Reelin for placement. Together, Reelin is a crucial factor that control primary cilia orientation and apical localization in principal neurons, and the cilia directionality of principal neurons is closely connected with cortical lamination.

How does Reelin Affect Directional Cilia Orientation of Principal Neurons?

How does Reelin influences the apical localization and directional orientation of primary cilia in principal neurons in inside-out laminated regions? Results from this study, together with our previous research (Yang et al., 2025), support a model in which Reelin guides embryonic neuronal migration toward the pial surface, which leads to accumulation of late-born neurons in the outer layers beneath the marginal zone. During postnatal development, due to crowding, late-born neurons undergo a slow reverse soma movement to inner regions. Early-born neurons in the deep layers may be passively influenced by late-born neurons to move backwards. This results in directional cilia orientation most prominently in late-born neurons, less in early-born neurons, and absent in atypical pyramidal neurons in the deep cortex. The model also predicts that during cortical evolution, increased production and migration of late-born neurons to the outer layer in a mammalian species would strengthen the reverse movement and result in a higher proportion of cortical neurons exhibiting directional cilia orientation toward the pia.

References:

Alexander, A., J. Herz, and L. Calvier. 2023. Reelin through the years: From brain development to inflammation. *Cell Rep*. 42:112669.

Bangs, F., and K.V. Anderson. 2017. Primary Cilia and Mammalian Hedgehog Signaling. *Cold Spring Harb Perspect Biol*. 9.

Barbas, H. 2015. General cortical and special prefrontal connections: principles from structure to function. *Annu Rev Neurosci*. 38:269-289.

Bishop, G.A., N.F. Berbari, J. Lewis, and K. Mykytyn. 2007. Type III adenylyl cyclase localizes to primary cilia throughout the adult mouse brain. *J Comp Neurol*. 505:562-571.

Blackstad, J.S., K.K. Osen, and T.B. Leergaard. 2022. The fibro- and cyto-architecture demarcating the border between the dentate gyrus and CA3 in sheep (Ovis aries) and domestic pig (Sus scrofa domesticus). *Hippocampus*. 32:639-659.

Breunig, J.J., M.R. Sarkisian, J.I. Arellano, Y.M. Morozov, A.E. Ayoub, S. Sojitra, B. Wang, R.A. Flavell, P. Rakic, and T. Town. 2008. Primary cilia regulate hippocampal neurogenesis by mediating sonic hedgehog signaling. *Proc Natl Acad Sci U S A*. 105:13127-13132.

Causeret, F., M.X. Moreau, A. Pierani, and O. Blanquie. 2021. The multiple facets of Cajal-Retzius neurons. *Development*. 148.

Chai, X., and M. Frotscher. 2016. How does Reelin signaling regulate the neuronal cytoskeleton during migration? *Neurogenesis (Austin)*. 3:e1242455.

Chen, X., J. Luo, Y. Leng, Y. Yang, L.S. Zweifel, R.D. Palmiter, and D.R. Storm. 2016. Ablation of type III adenylyl cyclase in mice causes reduced neuronal activity, altered sleep pattern, and depression-like phenotypes. *Biol Psychiatry*. 80:836-848.

Cooper, J.A. 2008. A mechanism for inside-out lamination in the neocortex. *Trends Neurosci*. 31:113-119.

Curran, T., G. D'Arcangelo, and A. Goffinet. 1995. Reeler gene discrepancies. *Nat Genet*. 11:12-13.

D'Arcangelo, G., G.G. Miao, S.C. Chen, H.D. Soares, J.I. Morgan, and T. Curran. 1995. A protein related to extracellular matrix proteins deleted in the mouse mutant reeler. *Nature*. 374:719-723.

Das, R.M., and K.G. Storey. 2014. Apical abscission alters cell polarity and dismantles the primary cilium during neurogenesis. *Science*. 343:200-204.

Elorriaga, V., A. Pierani, and F. Causeret. 2023. Cajal-retzius cells: Recent advances in identity and function. *Curr Opin Neurobiol*. 79:102686.

Falconer, D.S. 1951. Two new mutants, 'trembler' and 'reeler', with neurological actions in the house mouse (Mus musculus L.). *J Genet*. 50:192-201.

Frotscher, M., X. Chai, H.H. Bock, C.A. Haas, E. Forster, and S. Zhao. 2009. Role of Reelin in the development and maintenance of cortical lamination. *J Neural Transm (Vienna)*. 116:1451-1455.

Green, J.A., and K. Mykytyn. 2014. Neuronal primary cilia: an underappreciated signaling and sensory organelle in the brain. *Neuropsychopharmacology*. 39:244-245.

Hasenpusch-Theil, K., and T. Theil. 2021. The multifaceted roles of primary cilia in the development of the cerebral cortex. *Front Cell Dev Biol*. 9:630161.
Hattori, M. 2025. Regulatory mechanism of Reelin activity: a platform for exploiting Reelin as a therapeutic agent. *Front Mol Neurosci*. 18:1546083.
Hevner, R.F., T. Neogi, C. Englund, R.A. Daza, and A. Fink. 2003. Cajal-Retzius cells in the mouse: transcription factors, neurotransmitters, and birthdays suggest a pallial origin. *Brain Res Dev Brain Res*. 141:39-53.
Ho, E.K., and T. Stearns. 2021. Hedgehog signaling and the primary cilium: implications for spatial and temporal constraints on signaling. *Development*. 148.
Hoffarth, R.M., J.G. Johnston, L.A. Krushel, and D. van der Kooy. 1995. The mouse mutation reeler causes increased adhesion within a subpopulation of early postmitotic cortical neurons. *J Neurosci*. 15:4838-4850.
Howell, B.W., R. Hawkes, P. Soriano, and J.A. Cooper. 1997. Neuronal position in the developing brain is regulated by mouse disabled-1. *Nature*. 389:733-737.
Ishii, K., K.I. Kubo, and K. Nakajima. 2016. Reelin and Neuropsychiatric Disorders. *Front Cell Neurosci*. 10:229.
Jang, J., Y. Wang, M.A. Lalli, E. Guzman, S.E. Godshalk, H. Zhou, and K.S. Kosik. 2016. Primary Cilium-Autophagy-Nrf2 (PAN) Axis Activation Commits Human Embryonic Stem Cells to a Neuroectoderm Fate. *Cell*. 165:410-420.
Joly-Amado, A., N. Kulkarni, and K.R. Nash. 2023. Reelin Signaling in Neurodevelopmental Disorders and Neurodegenerative Diseases. *Brain Sci*. 13.
Jossin, Y. 2020. Reelin Functions, Mechanisms of Action and Signaling Pathways During Brain Development and Maturation. *Biomolecules*. 10.
Kajita, Y., and H. Mushiake. 2021. Heterogeneous GAD65 expression in subtypes of GABAergic neurons across layers of the cerebral cortex and hippocampus. *Front Behav Neurosci*. 15:750869.
Katsuyama, Y., and M. Hattori. 2024. REELIN ameliorates Alzheimer's disease, but how? *Neurosci Res*. 208:8-14.
Klingler, E. 2017. Development and Organization of the Evolutionarily Conserved Three-Layered Olfactory Cortex. *eNeuro*. 4.
Kohwi, M., and C.Q. Doe. 2013. Temporal fate specification and neural progenitor competence during development. *Nat Rev Neurosci*. 14:823-838.
Krubitzer, L.A., and A.M. Seelke. 2012. Cortical evolution in mammals: the bane and beauty of phenotypic variability. *Proc Natl Acad Sci U S A*. 109 Suppl 1:10647-10654.
Kupferman, J.V., J. Basu, M.J. Russo, J. Guevarra, S.K. Cheung, and S.A. Siegelbaum. 2014. Reelin signaling specifies the molecular identity of the pyramidal neuron distal dendritic compartment. *Cell*. 158:1335-1347.
Landrieu, P., and A. Goffinet. 1981. Inverted pyramidal neurons and their axons in the neocortex of reeler mutant mice. *Cell Tissue Res*. 218:293-301.
LeDoux, J. 2007. The amygdala. *Curr Biol*. 17:R868-874.
Lee, J.E., and J.G. Gleeson. 2011. Cilia in the nervous system: linking cilia function and neurodevelopmental disorders. *Curr Opin Neurol*. 24:98-105.
Macarelli, V., E. Leventea, and F.T. Merkle. 2023. Regulation of the length of neuronal primary cilia and its potential effects on signalling. *Trends Cell Biol*. 33:979-990.
Marin, O., and J.L. Rubenstein. 2003. Cell migration in the forebrain. *Annu Rev Neurosci*. 26:441-483.

Martin-Lopez, E., K. Ishiguro, and C.A. Greer. 2019. The Laminar Organization of Piriform Cortex Follows a Selective Developmental and Migratory Program Established by Cell Lineage. *Cereb Cortex*. 29:1-16.
Matsuki, T., R.T. Matthews, J.A. Cooper, M.P. van der Brug, M.R. Cookson, J.A. Hardy, E.C. Olson, and B.W. Howell. 2010. Reelin and stk25 have opposing roles in neuronal polarization and dendritic Golgi deployment. *Cell*. 143:826-836.
Mukhopadhyay, S., and R. Rohatgi. 2014. G-protein-coupled receptors, Hedgehog signaling and primary cilia. *Semin Cell Dev Biol*. 33:63-72.
Niehrs, C., F. Da Silva, and C. Seidl. 2025. Cilia as Wnt signaling organelles. *Trends Cell Biol*. 35:24-32.
Ogawa, M., T. Miyata, K. Nakajima, K. Yagyu, M. Seike, K. Ikenaka, H. Yamamoto, and K. Mikoshiba. 1995. The reeler gene-associated antigen on Cajal-Retzius neurons is a crucial molecule for laminar organization of cortical neurons. *Neuron*. 14:899-912.
Pal, K., and S. Mukhopadhyay. 2015. Primary cilium and sonic hedgehog signaling during neural tube patterning: role of GPCRs and second messengers. *Dev Neurobiol*. 75:337-348.
Phua, S.C., S. Chiba, M. Suzuki, E. Su, E.C. Roberson, G.V. Pusapati, S. Schurmans, M. Setou, R. Rohatgi, J.F. Reiter, K. Ikegami, and T. Inoue. 2019. Dynamic remodeling of membrane composition drives cell cycle through primary cilia excision. *Cell*. 178:261.
Rice, D.S., and T. Curran. 2001. Role of the reelin signaling pathway in central nervous system development. *Annu Rev Neurosci*. 24:1005-1039.
Rugarli, E.I., and A. Ballabio. 1995. Reelin: a novel extracellular matrix protein involved in brain lamination. *Bioessays*. 17:832-834.
Sasai, N., and J. Briscoe. 2012. Primary cilia and graded Sonic Hedgehog signaling. *Wiley Interdiscip Rev Dev Biol*. 1:753-772.
Sheldon, M., D.S. Rice, G. D'Arcangelo, H. Yoneshima, K. Nakajima, K. Mikoshiba, B.W. Howell, J.A. Cooper, D. Goldowitz, and T. Curran. 1997. Scrambler and yotari disrupt the disabled gene and produce a reeler-like phenotype in mice. *Nature*. 389:730-733.
Shepherd, G.M., and T.B. Rowe. 2017. Neocortical Lamination: Insights from Neuron Types and Evolutionary Precursors. *Front Neuroanat*. 11:100.
Singla, V., and J.F. Reiter. 2006. The primary cilium as the cell's antenna: signaling at a sensory organelle. *Science*. 313:629-633.
Sipos, E., S. Komoly, and P. Acs. 2018. Quantitative Comparison of Primary Cilia Marker Expression and Length in the Mouse Brain. *J Mol Neurosci*. 64:397-409.
Soriano, E., and J.A. Del Rio. 2005. The cells of cajal-retzius: still a mystery one century after. *Neuron*. 46:389-394.
Steger, R., L. Blachorsky, Q. Yang, and J.C. Brumberg. 2018. Synaptic properties of layer VI inverted pyramidal cells in the rodent somatosensory cortex. *Somatosens Mot Res*. 35:33-44.
Steger, R.M., R.L. Ramos, R. Cao, Q. Yang, C.C. Chen, J. Dominici, and J.C. Brumberg. 2013. Physiology and morphology of inverted pyramidal neurons in the rodent neocortex. *Neuroscience*. 248:165-179.
Sterpka, A., and X. Chen. 2018. Neuronal and astrocytic primary cilia in the mature brain. *Pharmacol Res*. 137:114-121.
Sterpka, A., J. Yang, M. Strobel, Y. Zhou, C. Pauplis, and X. Chen. 2020. Diverged morphology changes of astrocytic and neuronal primary cilia under reactive insults. *Mol Brain*. 13:28.

Stranahan, A.M., J.R. Erion, and M. Wosiski-Kuhn. 2013. Reelin signaling in development, maintenance, and plasticity of neural networks. *Ageing Res Rev*. 12:815-822.
Su, C.Y., S.N. Bay, L.E. Mariani, M.J. Hillman, and T. Caspary. 2012. Temporal deletion of Arl13b reveals that a mispatterned neural tube corrects cell fate over time. *Development*. 139:4062-4071.
Trommsdorff, M., M. Gotthardt, T. Hiesberger, J. Shelton, W. Stockinger, J. Nimpf, R.E. Hammer, J.A. Richardson, and J. Herz. 1999. Reeler/Disabled-like disruption of neuronal migration in knockout mice lacking the VLDL receptor and ApoE receptor 2. *Cell*. 97:689-701.
Tschaikner, P., F. Enzler, O. Torres-Quesada, P. Aanstad, and E. Stefan. 2020. Hedgehog and Gpr161: Regulating cAMP Signaling in the Primary Cilium. *Cells*. 9.
Tu, H.Q., S. Li, Y.L. Xu, Y.C. Zhang, P.Y. Li, L.Y. Liang, G.P. Song, X.X. Jian, M. Wu, Z.Q. Song, T.T. Li, H.B. Hu, J.F. Yuan, X.L. Shen, J.N. Li, Q.Y. Han, K. Wang, T. Zhang, T. Zhou, A.L. Li, X.M. Zhang, and H.Y. Li. 2023. Rhythmic cilia changes support SCN neuron coherence in circadian clock. *Science*. 380:972-979.
Valente, E.M., R.O. Rosti, E. Gibbs, and J.G. Gleeson. 2014. Primary cilia in neurodevelopmental disorders. *Nat Rev Neurol*. 10:27-36.
Vuong, L.T., and M. Mlodzik. 2023. The complex relationship of Wnt-signaling pathways and cilia. *Curr Top Dev Biol*. 155:95-125.
Wang, C.E., and S.K. Ogden. 2025. G Protein-Coupled Receptor Signal Intersection at the Primary Cilium. *Bioessays*. 47:e70015.
Wilsch-Bräuninger, M., and W.B. Huttner. 2021. Primary cilia and centrosomes in neocortex development. *Front Neurosci*. 15:755867.
Yanardag, S., and E.N. Pugacheva. 2021. Primary Cilium Is Involved in Stem Cell Differentiation and Renewal through the Regulation of Multiple Signaling Pathways. *Cells*. 10.
Yang, J., S. Mirhosseiniardakani, L. Qiu, K. Bicja, A. Del Greco, K.J. Lin, M. Lyon, and X. Chen. 2025. Cilia directionality reveals a slow reverse movement of principal neurons for positioning and lamina refinement in the cerebral cortex. *Development*. 152.
Yoneshima, H., E. Nagata, M. Matsumoto, M. Yamada, K. Nakajima, T. Miyata, M. Ogawa, and K. Mikoshiba. 1997. A novel neurological mutant mouse, yotari, which exhibits reeler-like phenotype but expresses CR-50 antigen/reelin. *Neurosci Res*. 29:217-223.
Zhou, Y., L. Qiu, A. Sterpka, H. Wang, F. Chu, and X. Chen. 2019. Comparative Phosphoproteomic Profiling of Type III Adenylyl Cyclase Knockout and Control, Male, and Female Mice. *Front Cell Neurosci*. 13:34.

Table S1: Cilia Orientation and Intracellular Location in Brain Regions of WT and *reeler* Mice

Brain Regions or Cell Types	WT (P30)			*Reeler* (P30)		
	Cilia Orientation	Lemina Cell Density	Cilia/Centriole Location	Cilia Orientation	Lemina Cell Density	Cilia/Centriole Location
DG	Roughly opposite	Compact	Mainly apical	Random	Disorganized	Irregular
CA3	Not very clear	Compact	Roughly apical	Random	Disorganized	Irregular
Dorsal CA1	Opposite, mainly toward the pia	Compact	base of apical dendrite	Opposite	Compact, Split SP	Mainly base of apical dendrite, Some irregular,
Ventral CA1	Opposite, mainly toward the pia	Compact	base of apical dendrite	Opposite	Compact, Split SP	Mainly base of apical dendrite, Some irregular
Neocortex (Late-born)	Oriented to the pia	Sparse	base of apical dendrite	mostly Oriented to the pia	Inverted, partially affected	Mostly, base of apical dendrite, Some irregular
Neocortex (Early-born)	Oriented to the pia	Sparse	Mostly at base of apical dendrite	Random	Inverted Disorganized	Irregular
Piriform Cortex (Layer II)	Opposite	Compact	base of apical dendrite	Random	Inverted Disorganized	Irregular
Piriform Cortex (Layer III)	Orient to the pia	Sparse	base of apical dendrite	Random	Inverted Disorganized	Irregular
Cingulate Cortex	Orient to the pia	Compact /Sparse	base of apical dendrite	Random	Inverted Disorganized	Irregular
CA1 Interneurons	Irregular	Not layered	Irregular	Irregular	Not layered	Irregular
Neocortex Interneurons	Irregular	Not layered	Irregular	Irregular	Not layered	Irregular
CA1 Astrocytes	Irregular	Not layered	Irregular	Irregular	Not layered	Irregular
Neocortex Astrocytes	Irregular	Not layered	Irregular	Irregular	Not layered	Irregular
Thalamus	Irregular	Not layered	Irregular	Irregular	Not layered	Irregular
Hypothalamus	Irregular	Not layered	Irregular	Irregular	Not layered	Irregular
Amygdala	Irregular	Not layered	Irregular	Irregular	Not layered	Irregular
Striatum	Irregular	Not layered	Irregular	Irregular	Not layered	Irregular

Table S2: Cilia Length in Various Brain Regions and Cell Types of WT and *reeler* Mice

Brain Region	Layering	P14		P30	
		WT (µm)	*reeler* (µm)	WT (µm)	*reeler* (µm)
CA1	Laminated	5.21 ± 0.36	5.86 ± 0.18 (*)	5.38 ± 0.33	8.62 ± 0.88 (***)
CA3	Laminated	5.13 ± 0.24	5.72 ± 0.14 (*)	5.32 ± 0.27	7.04 ± 0.22 (***)
DG	Laminated	2.82 ± 0.13	3.64 ± 0.16 (**)	2.90 ± 0.15	5.02 ± 0.20 (***)
Deep Neocortex	Laminated	4.31 ± 0.10	4.82 ± 0.20 (*)	4.49 ± 0.17	5.92 ± 0.10 (***)
Superficial Neocortex	Laminated	5.23 ± 0.11	5.71 ± 0.07 (**)	5.36 ± 0.07	6.88 ± 0.20 (***)
Piriform Cortex	Laminated	4.61 ± 0.25	5.12 ± 0.13 (*)	4.83 ± 0.09	6.02 ± 0.27 (**)
Entorhinal Cortex	Laminated	4.80 ± 0.27	5.33 ± 0.11 (*)	5.15 ± 0.14	6.01 ± 0.08 (***)
Thalamus	Non-laminated	ND	ND	5.53 ± 0.32	5.53 ± 0.34 (n.s.)
Hypothalamus	Non-laminated	ND	ND	5.48 ± 0.35	5.53 ± 0.33 (n.s.)
Amygdala	Non-laminated	ND	ND	5.28 ± 0.14	5.29 ± 0.16 (n.s.)
Striatum	Non-laminated	ND	ND	6.41 ± 1.02	6.43 ± 1.01 (n.s.)
Astrocyte CA1	Non-laminated	ND	ND	5.12 ± 0.01	5.14 ± 0.03 (n.s.)
Astrocyte deep cortex	Non-laminated	ND	ND	4.25 ± 0.14	4.34 ± 0.11 (n.s.)
Astrocyte Superficial Cortex	Non-laminated	ND	ND	4.51 ± 0.07	4.50 ± 0.06 (n.s.)
Interneuron CA1	Non-laminated	ND	ND	5.09 ± 0.11	5.13 ± 0.14 (n.s.)
Interneuron Deep Cortex	Non-laminated	ND	ND	5.13 ± 0.19	5.11 ± 0.10 (n.s.)
Interneuron Superficial Cortex	Non-laminated	ND	ND	5.16 ± 0.34	5.17 ± 0.31 (n.s.)

Figure and Figure Legends:

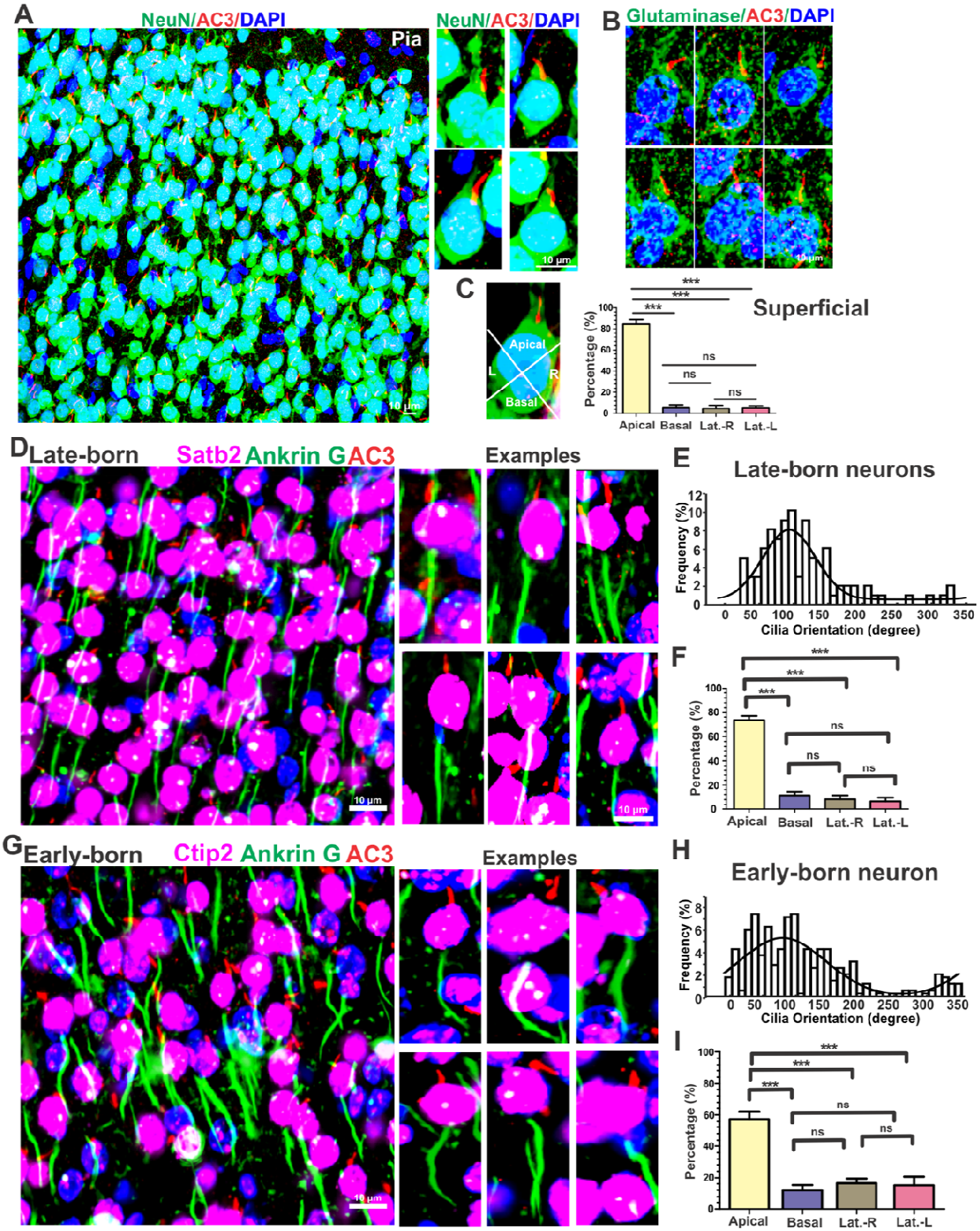

Figure 1

Fig. 1. Primary cilia of neocortical principal neurons are predominantly localized near the base of apical dendrites and aligned opposite to the AIS. (A-C) Representative images showing cilia orientation and cilia location in the superficial layer. **(A-B)** Neurons marked by NeuN and Glutaminase antibodies. **(C)** (Left) A diagram showing how four quadrants (Apical, Basal, Lateral-Right and Lateral-Left) was defined in reference to the center of nucleus and apical dendrite. The location of cilia base in a quadrant was used to determine cilia location. (Right) Cilia predominantly localize to the apical quadrant in superficial neocortical neurons. **(D-F)** Late-born neurons cilia orientation and subcellular location. **(D)** Representative images showing cilia aligned opposite to AIS relative to the nuclei. **(E)** Cilia orientation histogram. **(F)** Cilia of late-born neurons were predominantly distributed to the apical quadrant. **(G-I)** Early-born neurons cilia orientation and location. **(H)** Cilia orientation histogram. **(I)** Cilia of early-born neurons were mostly distributed to the apical quadrant, while many still dispersed to other quadrants. **E** and **H** were fitted with one or two periodic normal distribution density functions, combined with a uniform distribution. One-way ANOVA tests were used to compare groups in cilia location.

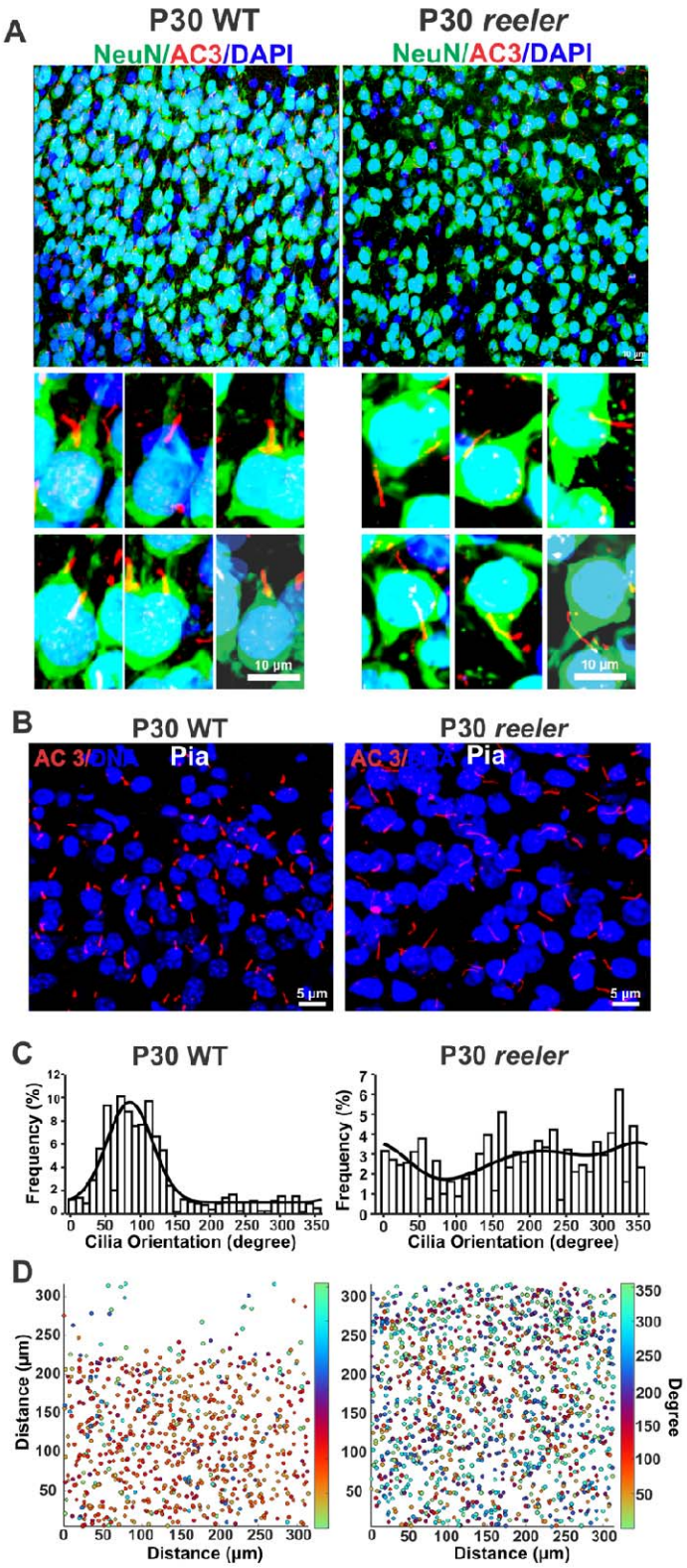
A
P30 WT
NeuN/AC3/DAPI
P30 reeler
NeuN/AC3/DAPI
10 µm
10 µm
B
P30 WT
AC 3/DNA
Pia
P30 reeler
AC 3/
Pia
5 µm
5 µm
C
P30 WT
Frequency (%)
Cilia Orientation (degree)
P30 reeler
Frequency (%)
Cilia Orientation (degree)
D
Distance (µm)
Distance (µm)
Distance (µm)
Degree

Figure 2

Fig. 2. Disrupted directional cilia orientation in the outer layer of the *reeler* neocortex. (A-B) Primary cilia in the outer layer of the WT and *reeler* neocortices. WT cilia were mostly localized to the apical dendrites and oriented to the pia, while *reeler* cilia were irregularly distributed and lacked preferred orientation. **(C)** Histograms of cilia orientations in the outer layers of the reeler neocortex. WT cilia oriented toward the pia (peak at ~90°), while *reeler* cilia did not. Data were fitted with one or two periodic normal distribution density functions, combined with a uniform distribution. **(D)** Orientation map in the outer layers visualizing cilia orientation across the sampled fields, color-coded by angle (degrees). Data were pooled from multiple sections out of multiple *reeler* and WT brains.

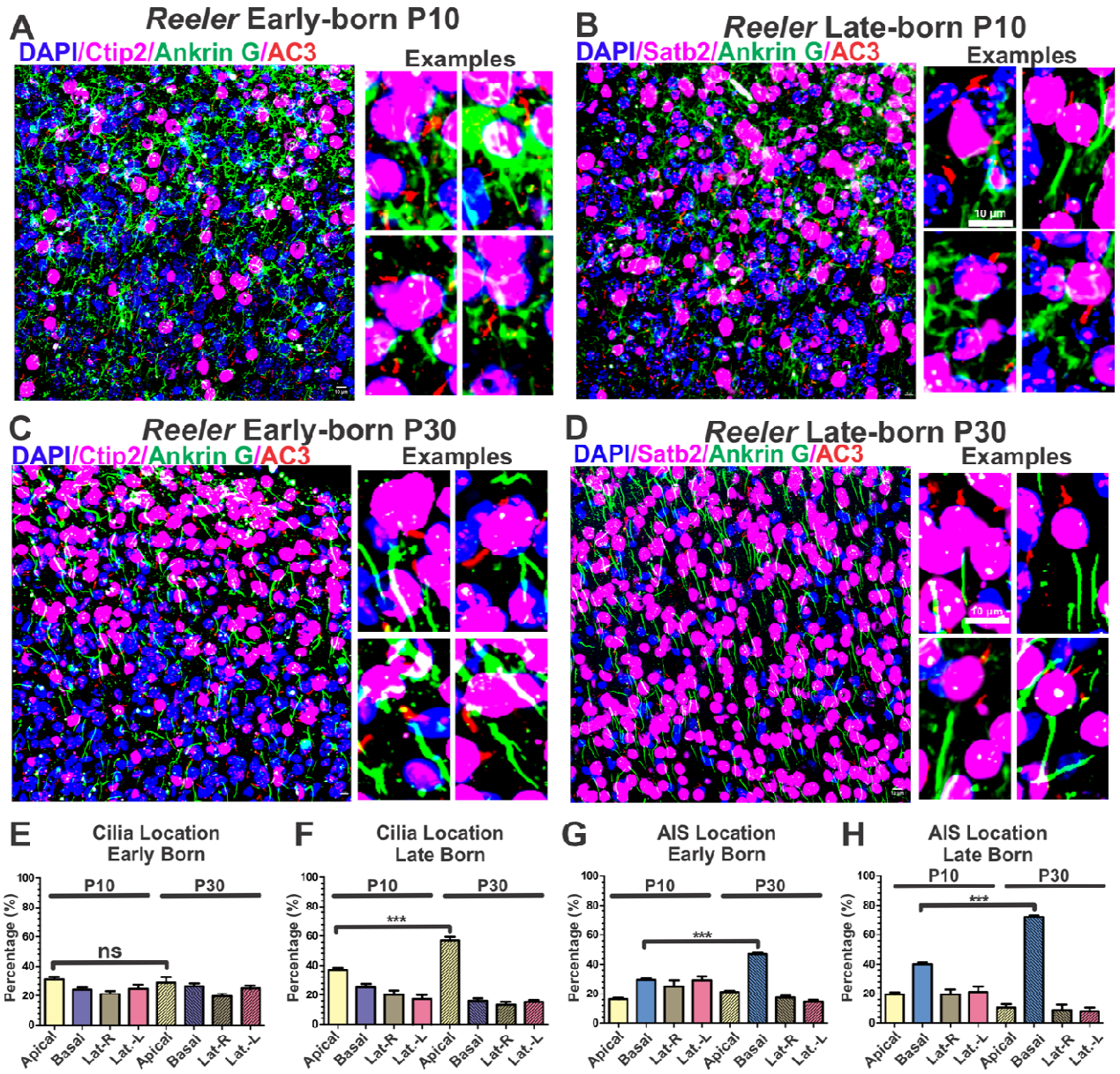

Figure 3

Fig. 3. *Reeler* late-born neurons exhibit a stronger postnatal rectification in apical-basal orientation than early-born neurons. *Reeler* early-born neurons **(A)** and late-born neurons **(B)** at P10; early-born neurons **(C)** and late-born neurons **(D)** at P30. Primary cilia, AIS, early- and late-born neurons were labeled by AC3, Ankyrin G, CTIP2, and Satb2 antibodies, respectively. **(E-H)** cilia and AIS distribution in four quadrants of P10 and P30. At P10, mis-localized cilia and axon present in both early- and late born neurons. At P30, most late-born neurons' cilia were localized to the apical quadrant and axons to the basal quadrant, while early-born neuron's cilia were randomly distributed to four quadrants.

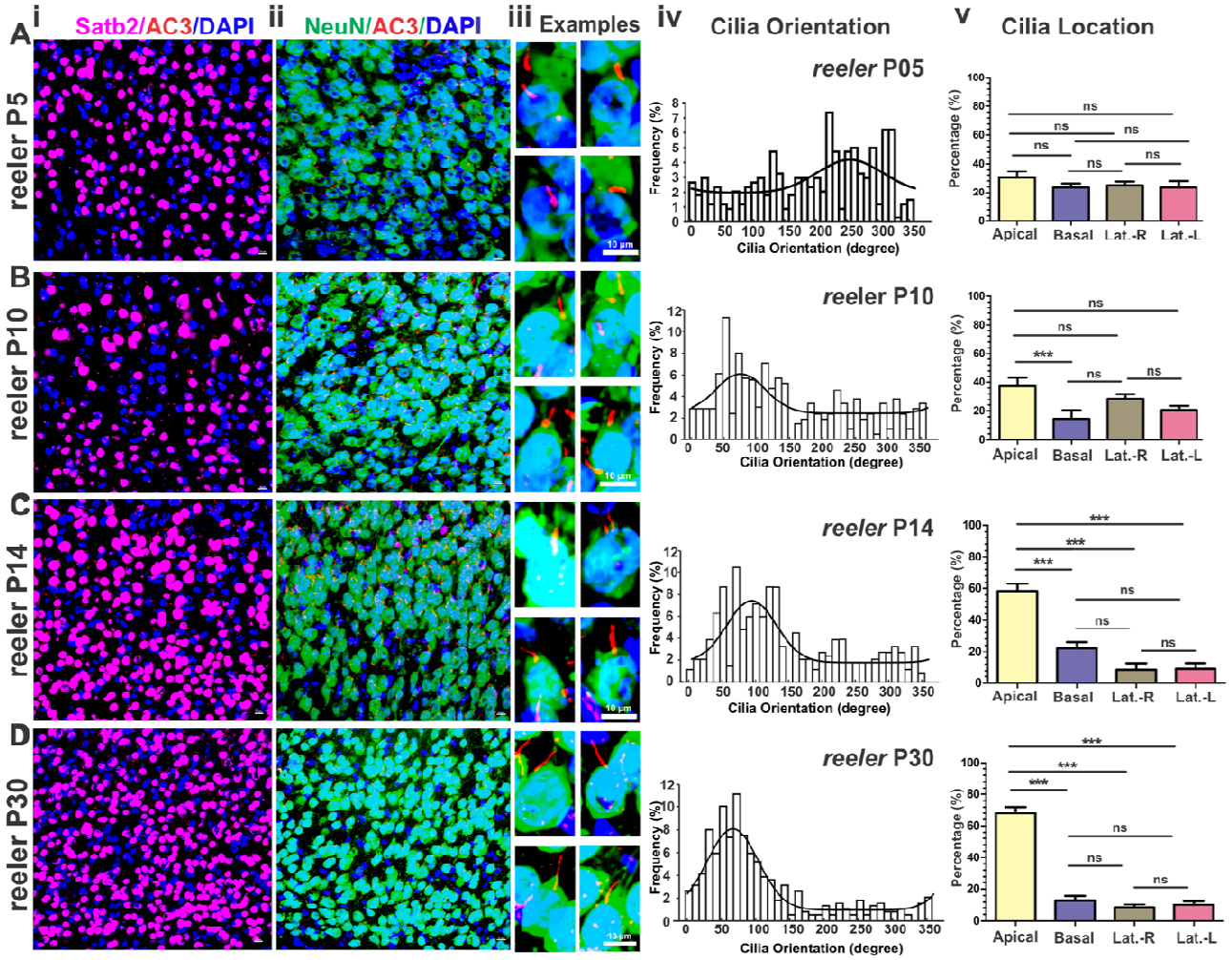

Figure 4

Fig. 4. *reeler* late-born neocortical neurons are subject to corrections in cilia orientation and cilia apical location during postnatal development. (A-D) *reeler* late-born neurons at P5 (**A**), P10 (**B**), P14 (**C**) and P30 (**D**). (**i**) Images of late-born neurons and primary cilia. (**ii**) Images of late-born neurons and cilia marked by NeuN and AC3 antibodies, respectively. NeuN staining display the apical dendrites. (**iii**) Representative images of individual neurons with apical dendrites and cilia. (**iv**) Cilia orientation of late-born neurons at different ages. Histograms of cilia orientation with fitting curves. (**v**) Cilia intracellular location in four quadrants at different ages. One-way ANOVA tests were used to compare groups.

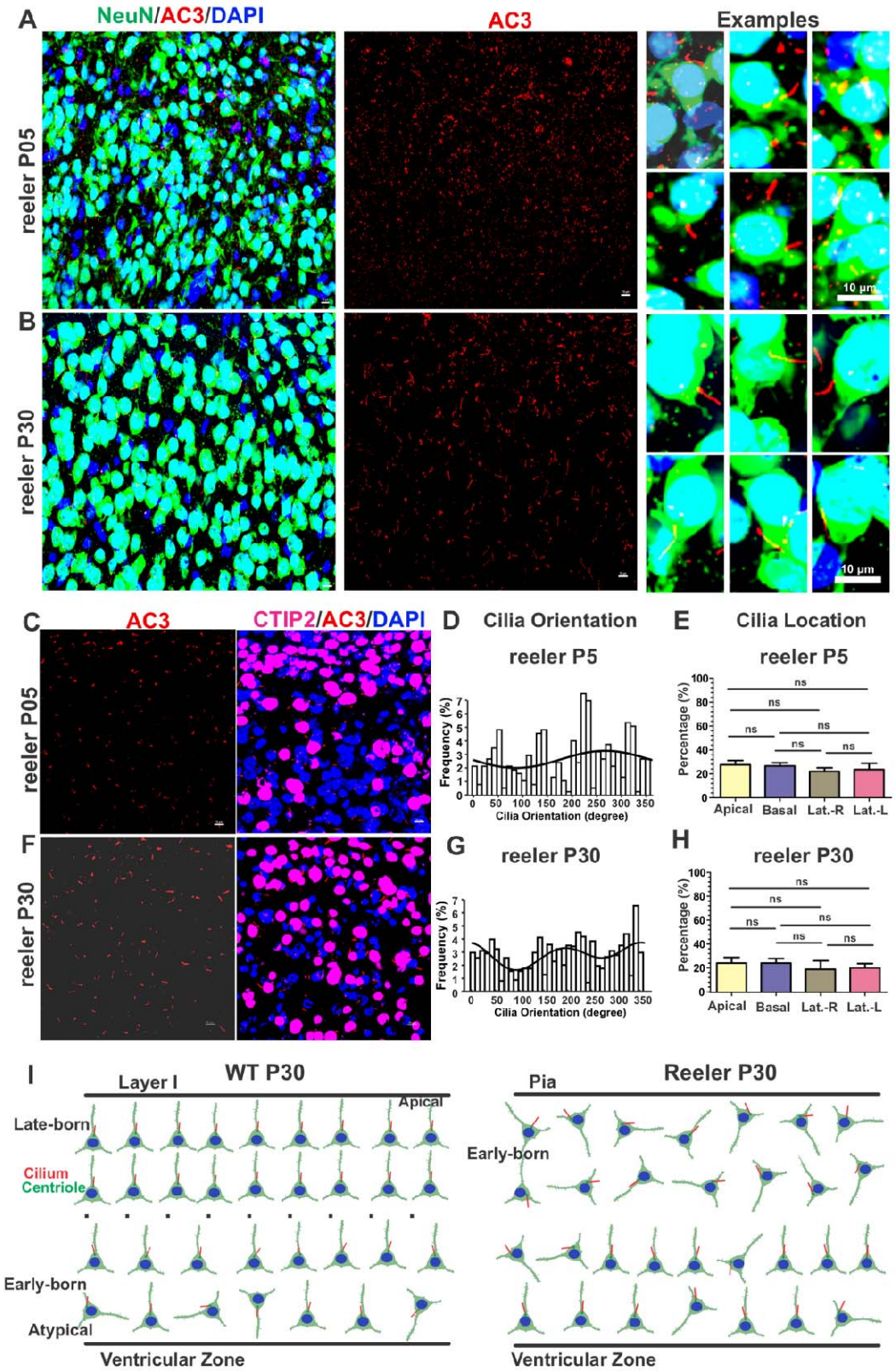
A
NeuN/AC3/DAPI
AC3
Examples
reeler P05
10 µm
B
reeler P30
10 µm
C
AC3
CTIP2/AC3/DAPI
reeler P05
D
Cilia Orientation
reeler P5
Frequency (%)
Cilia Orientation (degree)
E
Cilia Location
reeler P5
Percentage (%)
ns
Apical
Basal
Lat.-R
Lat.-L
F
reeler P30
G
reeler P30
H
reeler P30
I
Layer I
WT P30
Apical
Late-born
Cilium
Centriole
Early-born
Atypical
Ventricular Zone
Pia
Reeler P30
Early-born
Ventricular Zone

Figure 5

Fig. 5. *reeler* early-born neocortical neurons do not exhibit postnatal corrections in cilia orientation and apical location. (A-B) cilia of *reeler* early-born neurons at P5 **(A)** and P30 **(B)**. Cilia lack preferred orientation and apical location. Early-born *reeler* neurons at P5 **(C-E)** and P30 **(F-H)** were marked by a CTIP2 antibody. **(C - F)** Representative early-born neuron and cilia images. **(D** and **H)** Histogram of cilia orientation of early-born neurons. (**E - H**) Cilia intracellular location in four quadrants. One-way ANOVA tests were performed to compare groups. **(I)** Schematic diagrams depicting cilia orientation and intracellular location in neocortical principal neurons of WT and *reeler* at P30.

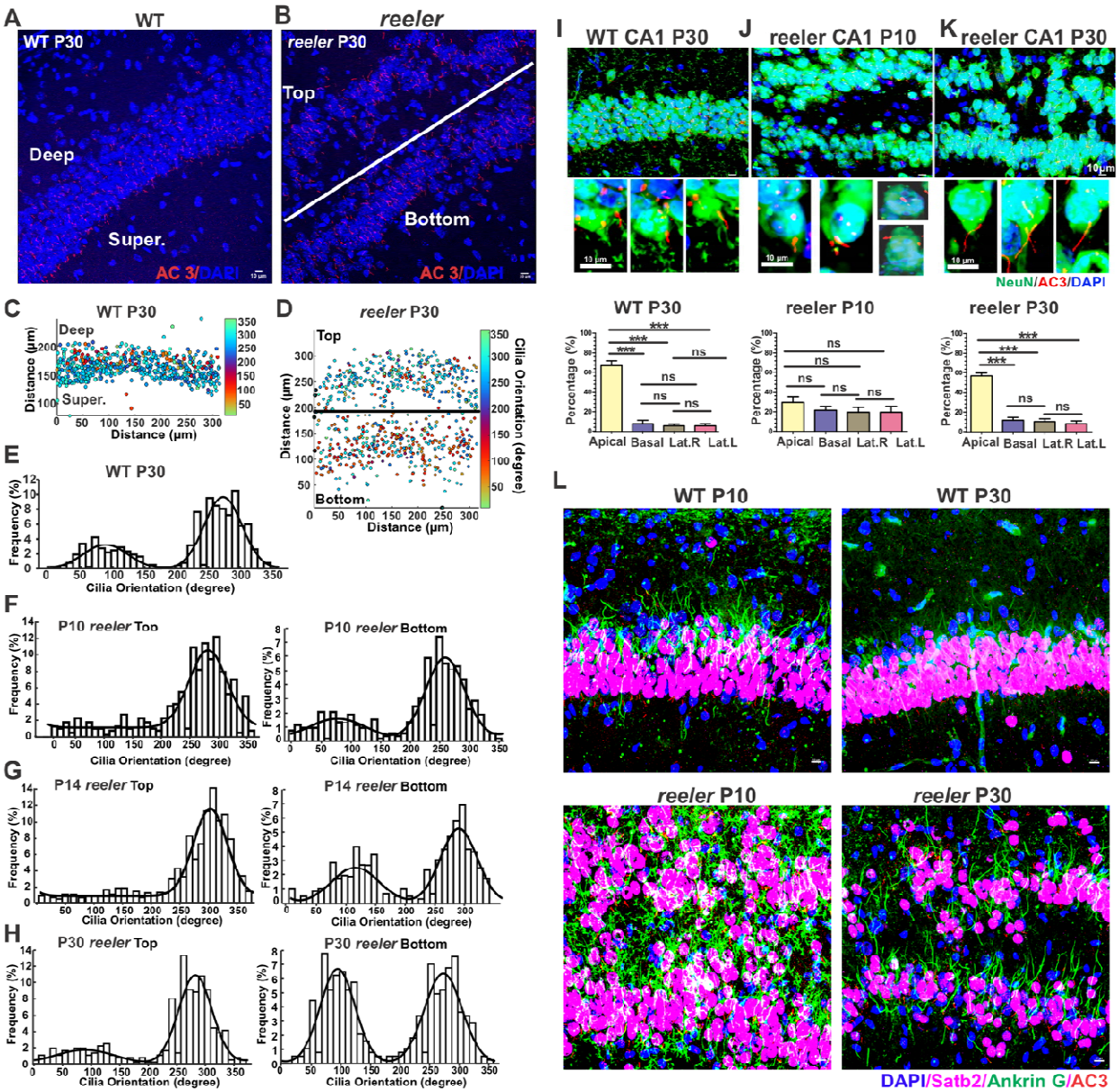

Figure 6

Fig. 6. Reelin deficiency partially alters cilia orientation and cilia apical localization in CA1 pyramidal neurons. (A-B) Representative images in WT (**A**) and *reeler* (**B**) CA1 regions at P30. *reeler* CA1 split "top" and "bottom". **(C-D)** Cilia orientation map in WT (**C**) and *reeler* CA1 (**D**), visualizing cilia orientation across the sampled fields, color-coded by angle (degrees). **(E)** Histogram of cilia orientation in WT CA1 at P30. **(F - H)** Histograms showing cilia orientation in the top and bottom of *reeler* at P10 (**F**), P14(**G**), and P30 (**H**), respectively. **(I-K)** WT at P30 (**I**), *reeler* P10 (**J**) and *reeler* P30 (**K**). Cilia location in *reeler* CA1 neurons rectified during postnatal development from P10 to P30. Top: Representative CA1 images; Middle: individual neurons. Bottom: cilia location in four quadrants. ANOVA tests **(L)** WT CA1 neurons clearly exhibit a cilia-at-apical and axon-at-basal pattern at both P10 and P30. *reeler* CA1 neurons manifest altered localization pattern at P10 but had corrections at P30.

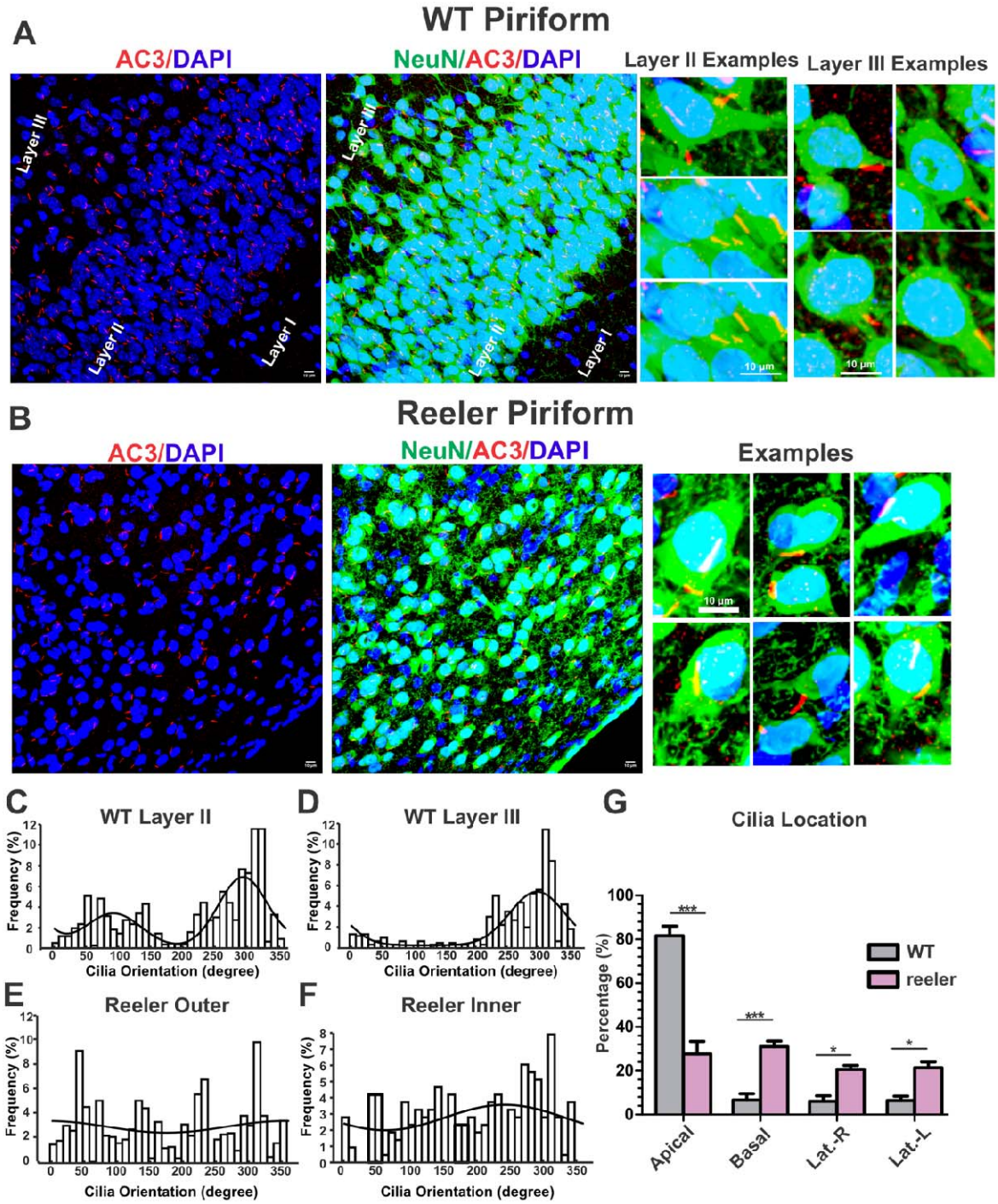

Figure 7

Fig. 7. Disrupted cilia orientation and apical localization in the *reeler* piriform cortex. WT **(A)** and *reeler* **(B)** piriform cortex of P30. Representative images of individual neurons are shown on the right. Histogram of cilia orientation in Layer II and III of WTs (**C-D**) and in outer and inner layers of reeler of P30 (**E-F**). **(G)** Percentage of cilia subcellular location in 4 quadrants. Cilia of WT neurons, but not *reelers*, primarily distribute to the apical quadrant.

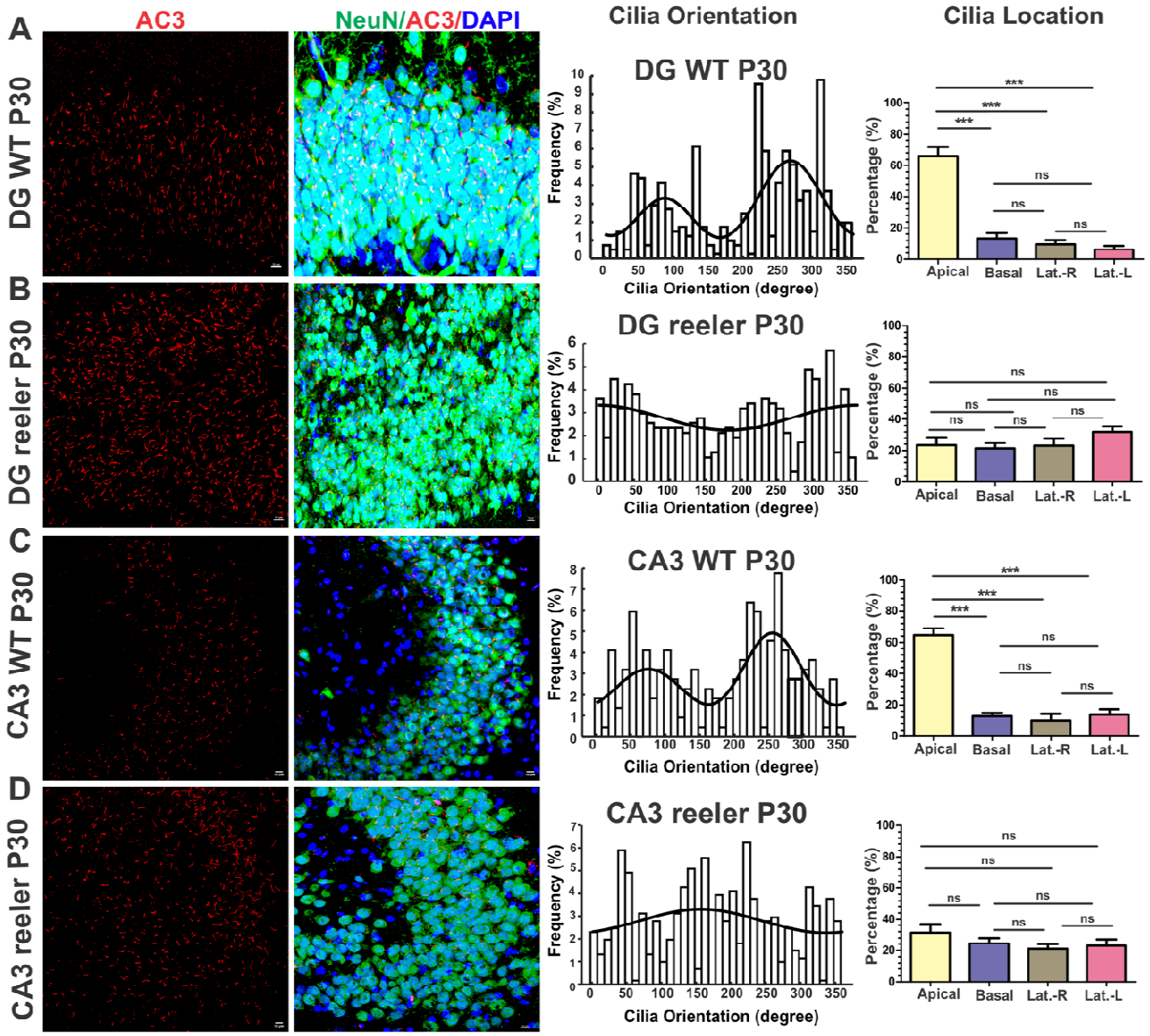

Figure 8

Fig. 8. Disrupted layering and ciliation pattern in the *reeler* DG and CA3. Representative neuron and cilia images, marked by NeuN and AC3 antibodies, respectively. Data were collected from P30 brain samples. Histograms of cilia orientation and cilia intracellular location in WT and *reeler* are shown on the right. The pattern of cilia orientation and cilia intracellular location in WT DG and CA3 were not as strong or easily distinguishable as neocortical neurons. However, the loss of Reelin clearly altered the preferred apical location of cilia in DG and CA3.

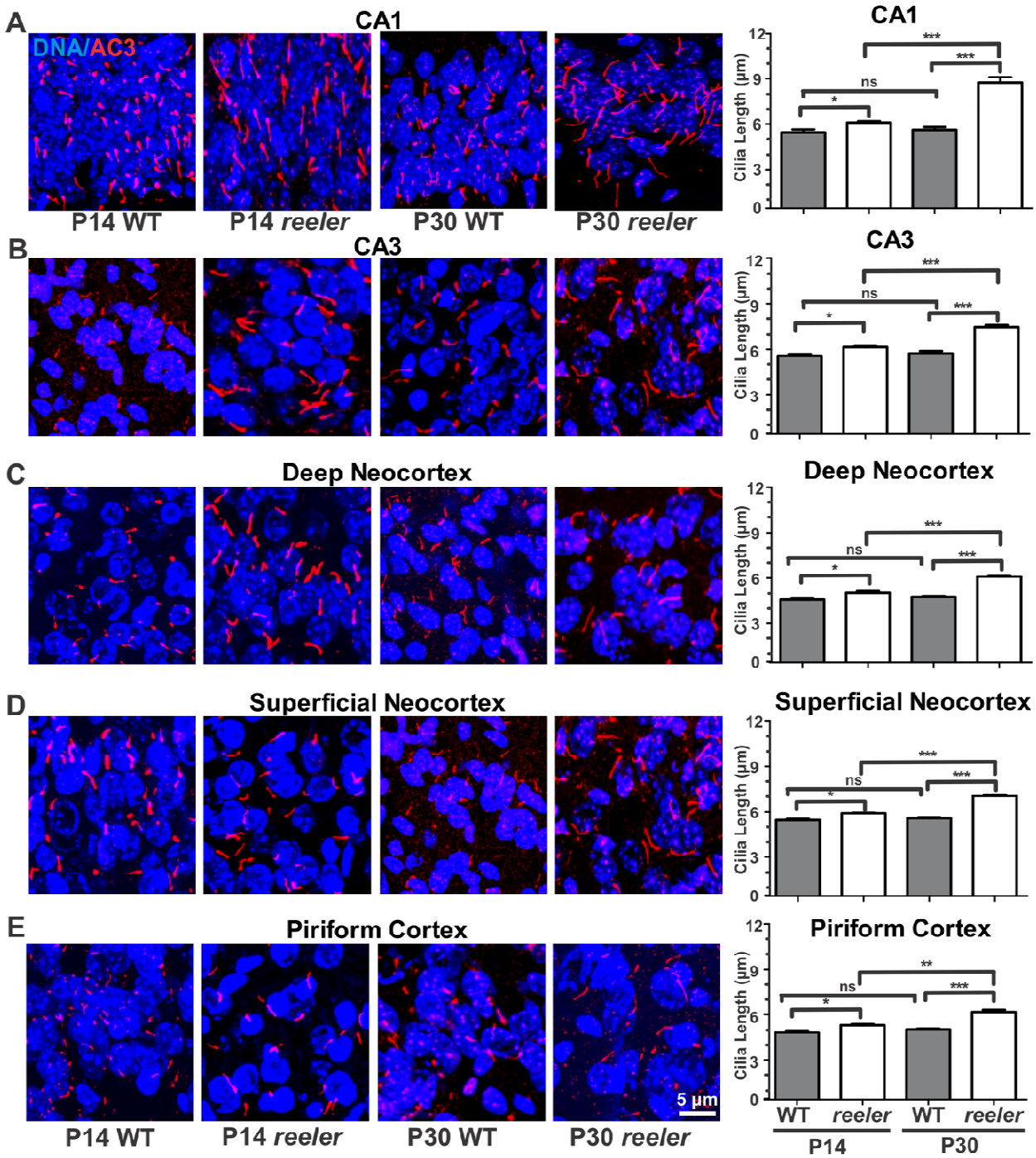

Figure 9

Fig. 9. Reelin deficiency promotes cilia elongation in principal neurons after P14 throughout the cerebral cortex. (**Left**) Representative images of neuronal primary cilia (marked by an AC3 antibody) in different brain regions of WT and *Reeler* at P14 and P30. (**Right**) Bar graph showing cilia length of P14 and P30 WT and *reeler* mice. **(A)** CA1; **(B)** CA3; **(C)** Deep Neocortex; **(D)** Superficial Neocortex; and **(E)** Piriform Cortex. Two-tailed Student's T-tests were performed to compare two groups.

Supplemental Figure Legends:

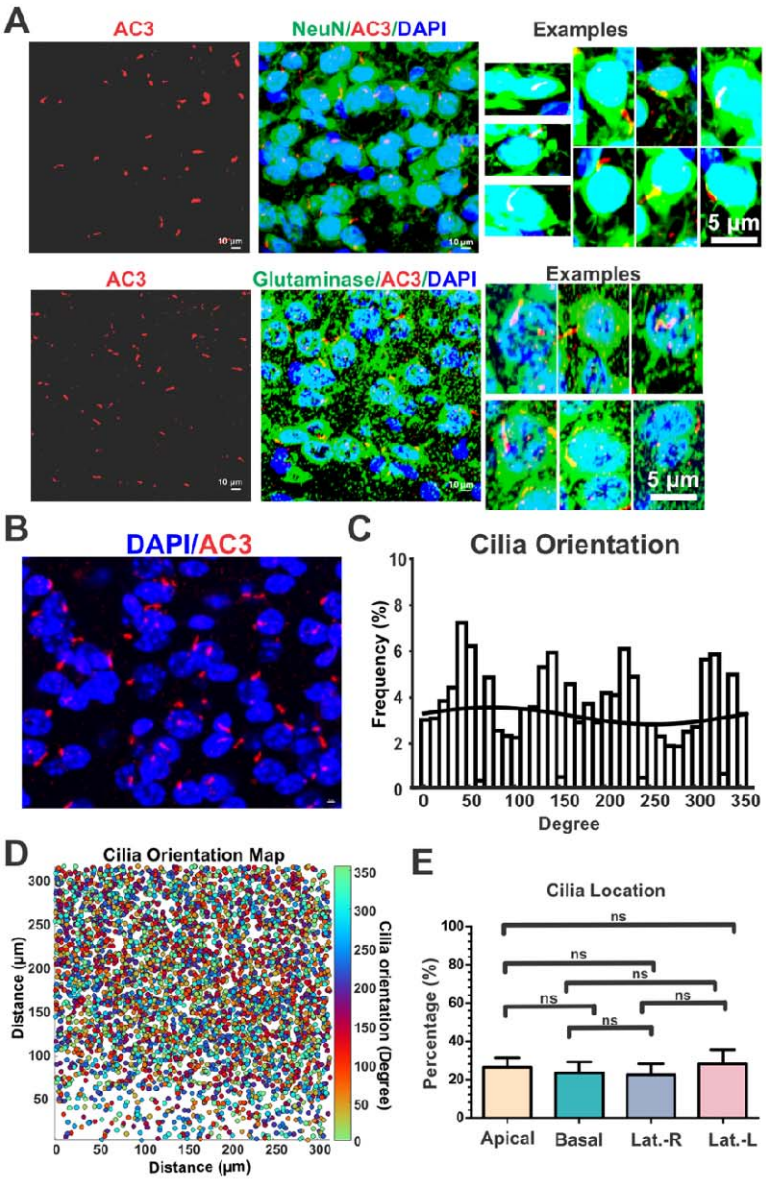

Fig. S1

Fig. S1. Irregular cilia orientation and random cilia location in atypical pyramidal neurons in the WT deep neocortex. (A) Representative image of atypical pyramidal neurons stained with NeuN antibody (Top) or Glutaminase I (Bottom). **(B)** Representative cilia images in the deep layer. **(C)** Histogram showing the frequency distribution of cilia orientation angles (0° - 360°), with a flattened fitting curve indicating random orientation. **(D)** Cilia orientation map of atypical pyramidal neurons visualizing cilia orientation across the sampled fields, color-coded by angle (degrees). Data were pooled from multiple brain sections out of multiple animals. **(E)** Cilia location in 4 quadrants of atypical pyramidal neurons. An ANOVA test was performed.

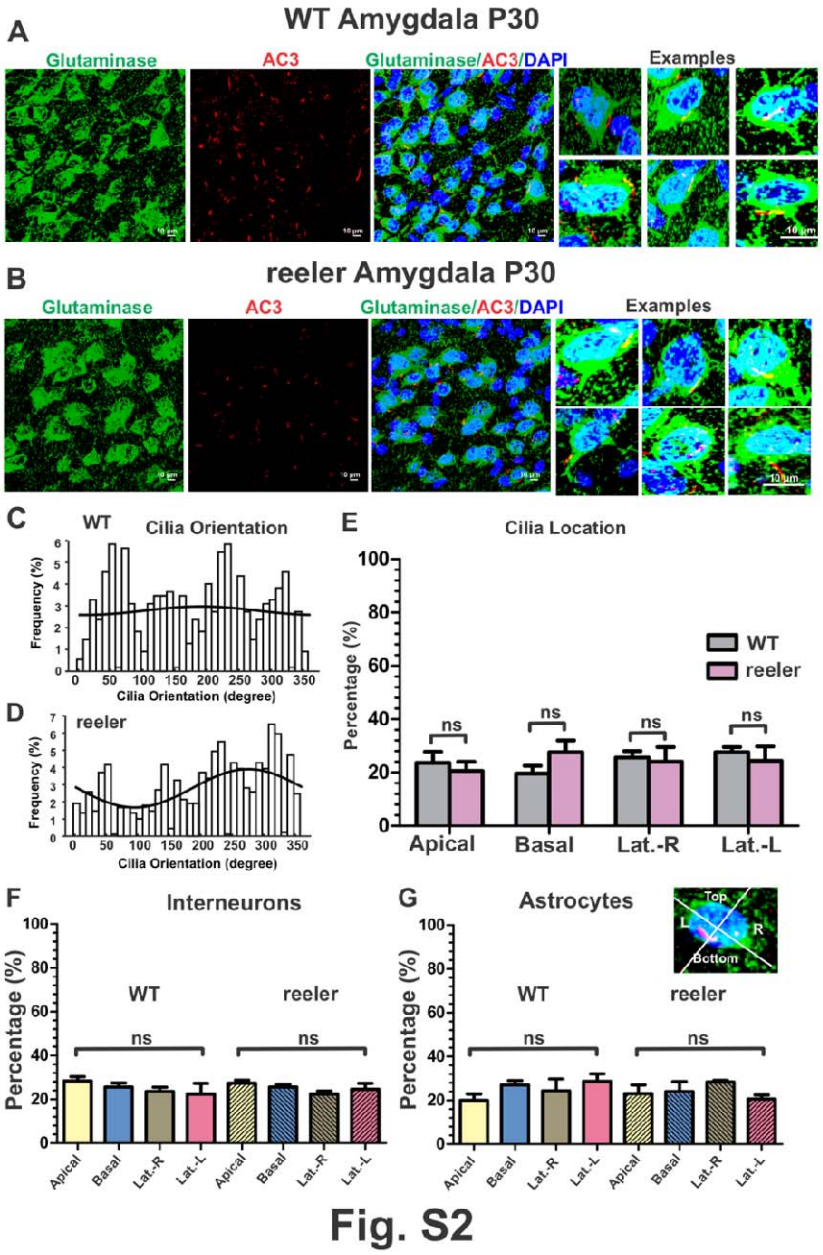

Fig. S2. (A-E) Primary cilia of excitatory neurons in the WT and *reeler* amygdala exhibit random orientation and irregular location. (A-B) Representative images of excitatory neurons, marked by a Glutaminase antibody, and in the WT **(A)** and *reeler* **(B**) amygdala**. (C-D)** Cilia orientation histogram shows the distribution of cilia orientation angles of excitatory neurons in the WT amygdala. **(E)** WT and *reeler* cilia subcellular location in 4 quadrants**.** In both genotypes, cilia orientations were distributed across the full 360° range without a dominant axis, indicating irregular alignment. **(F-G) Primary cilia were roughly evenly dispersed to 4 quadrants in WT and *reeler* interneurons and astrocytes, lacking a dominant distribution in subcellular localization**. Interneurons and astrocytes were marked by GAD65 and GFAP antibodies, respectively. Insert in G, a diagram showing how 4 quadrants in the soma (Top, Bottom, Lateral-Left and Lateral-Right) were defined in reference to the nucleus.

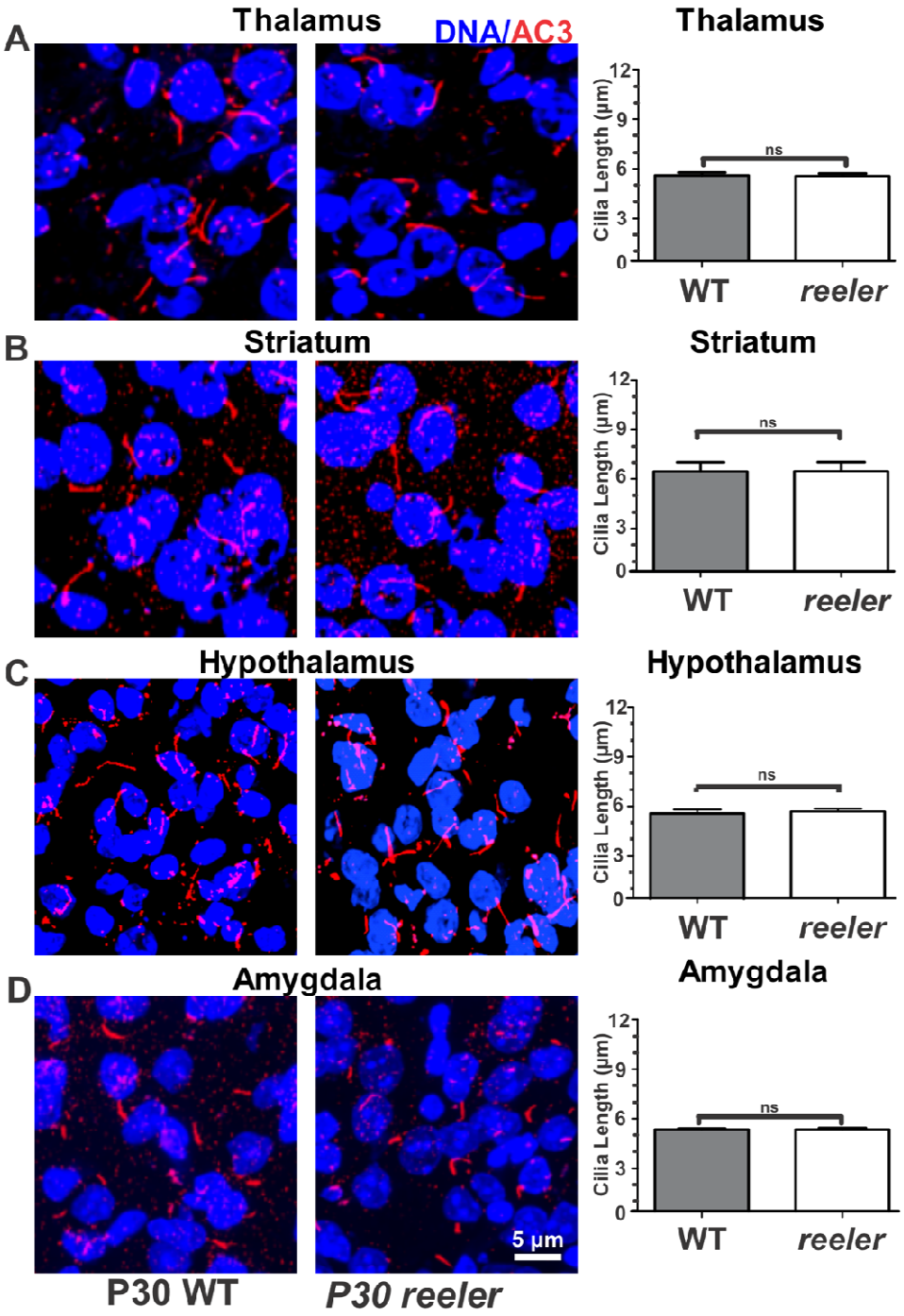

Fig. S3

Fig. S3. Reelin does not influence the cilia length of excitatory neurons in non-laminated brain regions. (A) Representative neuronal cilia images and bar graph showing comparable cilia length in the thalamus of WT and *reeler* mice at P30. Similar measurements in the striatum **(B)**, hypothalamus **(C)**, and amygdala **(D)** also showed no significant differences between genotypes. Student's T-test. ns, not significant.

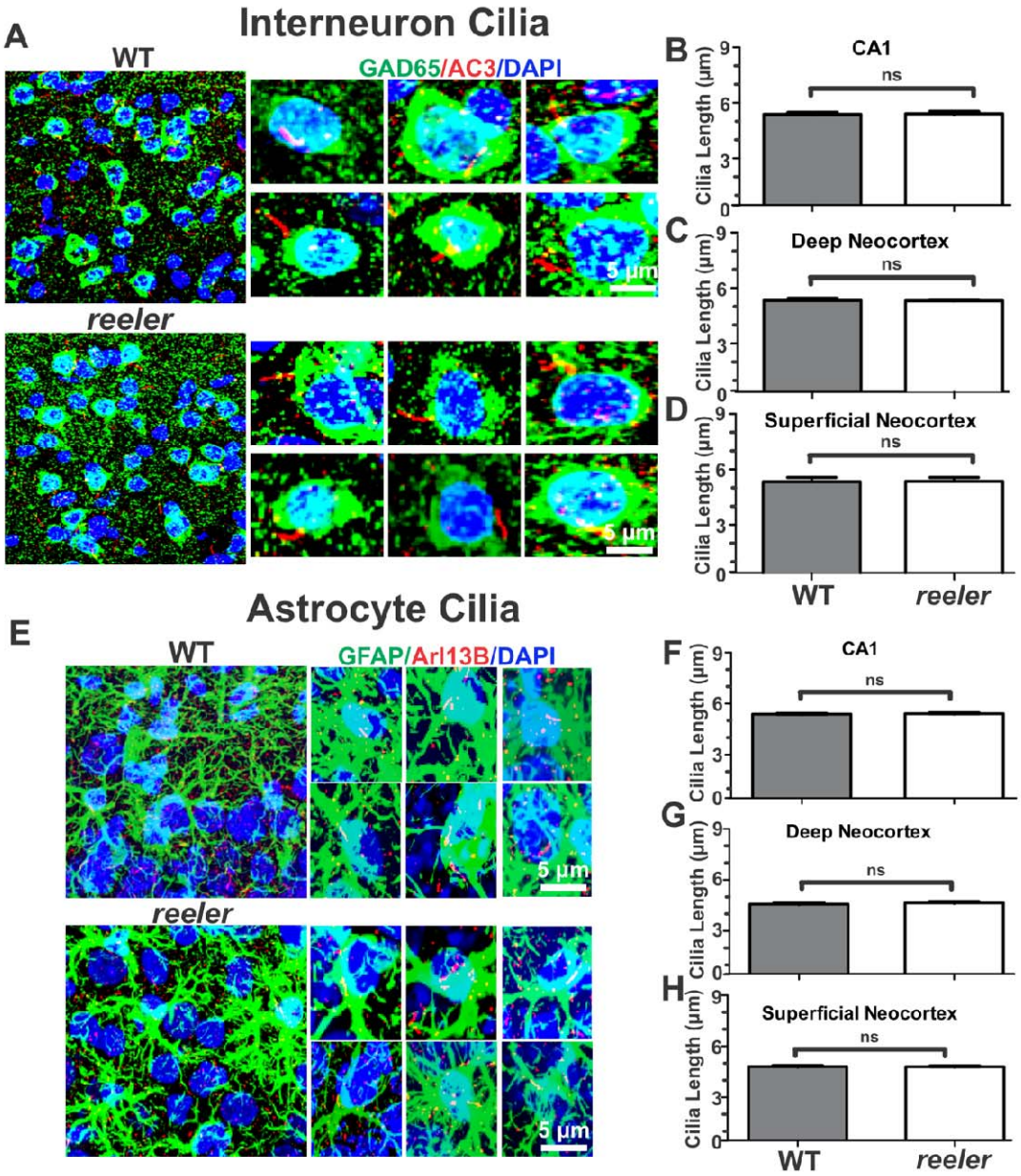

Fig. S4

Fig. S4. Reelin does not affect cilia length in interneurons or astrocytes. (A) Representative images and individual neurons and **(B-D)** bar graphs showing primary cilia length in interneurons of WT and *reeler* mice at P30. Interneurons were identified by a GAD65 antibody. Measurements in interneurons from the CA1 region (**B**), deep (**C**) and superficial (**D**) neocortex also revealed no significant differences between genotypes. **(E)** Representative confocal images and individual astrocytes and **(F-H)** bar graphs showing primary cilia length in astrocytes of WT and *reeler* mice at P30. Astrocytes were marked by a GFAP antibody. Measurements in astrocytes from the CA1 region (**F**), deep (**G**) and superficial (**H**) neocortex also revealed no significant differences between genotypes. Statistical analysis was performed using Student's T-test.